A Geologic Study of the Capulin Volcano National Monument and surrounding areas, Union and Colfax Counties, New Mexico

by

William O. Sayre and Michael H. Ort

New Mexico Bureau of Geology and Mineral Resources, New Mexico Tech
Socorro, New Mexico 87801

Open-file Report 541

August, 2011

A geologic study of Capulin Volcano National Monument and surrounding areas

Final Report
Cooperative Agreement CA7029-2-0017
December 4, 1999

Submitted to:

Capulin Volcano National Monument
P. O. Box 80
Capulin, New Mexico 88414

Submitted by:

William O. Sayre, Ph.D., P.G.
College of Santa Fe
1600 St. Michael's Drive
Santa Fe, New Mexico 87505-7634

and

Michael H. Ort, Ph.D.
Department of Geology
PO Box 4099
Northern Arizona University
Flagstaff, Arizona 86011

Table of Contents

Executive Summary

Capulin Volcano is a unique cinder cone in the National Park System. Its *boca*, or mouth, at its western flank, is more complex than most cinder cones. The volcano is very accessible, with a paved road to its rim, and it has become a well-established stop for both tourists and university geology field trips.

The eruption of Capulin volcano took place about 60,000 years ago over a period of a month to a few years. The first lava flows came out of small vents, followed by the eruption of cinder to make the volcanic edifice itself. After the cone grew to its present height, more lava was erupted from the western base of the volcano, forming the *boca* or mouth, consisting of several vents, lava lakes and lava tubes. These flows soon surrounded the volcano.

Introduction

Purpose of investigation

No original geologic baseline investigation of Capulin Volcano National Monument had ever been done before this project. Knowledge of the geologic history and geologic resources of the park were known only in broad terms. National Park Service (NPS) personnel were unable to verify even if a geologist had prepared the lava flow series map displayed in the park brochure. It seemed necessary to develop a much more accurate picture of the park's geology through a cooperative agreement with the College of Santa Fe.

Research Objectives

1. A geologic investigation of Capulin Volcano and surrounding areas, to include age determinations and a history of the eruption of Capulin volcano

2. Assist the park in improving and expanding public interpretive programs

3. Provide input into natural resource management issues

4. Assist in recognizing and mitigating potential threats to the National Monument

Conditions under which study was conducted

Dr. William O. Sayre and Dr. Michael H. Ort performed work at their offices in Arizona and New Mexico and in the field at Capulin Volcano National Monument. Work commenced in 1993 and finished in 1999. Fieldwork was done primarily during the summer of each year.

General plan of treatment of the subject

Our plan of work followed generally accepted standards for geologic field and laboratory work. We mapped geologic features, collected samples, and contracted for geochemical analyses and age determinations, the goal of which was to interpret the volcanic history of the park. Dr. Ort performed the paleomagnetic analyses. We used geographic information systems software to prepare the geologic map following procedures set out by the NPS Southwest Region GIS Center. The format of our reports followed the NPS Southwest Region Report Requirements.

Summary of previous work

Capulin Volcano is part of the Raton-Clayton volcanic field (RCVF) in northeastern New Mexico and southern Colorado. The RCVF is located in the Great Plains physiographic province near the Sangre de Cristo Mountains, a range of the Rocky Mountains.

<u>Geologic history of northeastern New Mexico</u>

Not much is known about the earliest history of this part of New Mexico. Rocks of Precambrian time, before 544 million years ago, are buried deeply. The University of New Mexico is planning to undertake seismic profiling of the area, but until that time we know little (Keller et al., 1999).

Rocks of most of the Paleozoic era, from the Cambrian to middle Carboniferous (end of the Mississippian) eras, or from 544 m.y. to 320 million years before present (m.y.b.p.), are also absent in northeastern New Mexico. This is due to the rise of the Sierra Grande Arch, a range of the Ancestral Rocky Mountains that formed during late Carboniferous time (or Pennsylvanian, from 320 m.y. to 300 m.y.b.p.) (Kent, 1972). The arch is named for the largest volcano in the RCVF, but it is completely unrelated to it, except that it is located in the same area. Sierra Grande Arch was composed of Precambrian rocks that were uplifted to elevations of several thousand feet. Any rocks deposited after the Precambrian and before the Pennsylvanian would have been eroded off of the rising mountain belt.

The modern-day Rocky Mountains provide us with a modern analogue of the Ancestral Rockies at their zenith. The Rockies are also composed of Precambrian rocks and stand in high relief over the surrounding landscape.

The arch began to erode during Pennsylvanian time and is now buried by younger sedimentary rocks to a depth of a few thousand feet. There may be a thin layer of Permian rocks (300 – 251 m.y.b.p.) deposited on top of Sierra Grande Arch similar in age to the reef limestones that make up Guadalupe Mountains National Park in west Texas, but these, too, are deeply buried. Thin layers of rocks of the Triassic and Jurassic periods of the Mesozoic era (251 m.y.b.p. to 142 m.y.b.p.) also blanket the Arch and the thin Permian cover (Woodward, 1987).

Rocks of the Cretaceous era (142 m.y.b.p. to 65 m.y.b.p.) were laid down on the older rocks and actually crop out on the landscape in the vicinity of Capulin Volcano. In particular, the Dakota Sandstone, a tan-colored rock, is found in outcrops along the road between Folsom and Des Moines, among other places.

The Cretaceous was an interesting era for western North America. A new range of mountains rose in the far west during the Sevier orogeny. In New Mexico and most of the rest of the west, a shallow sea formed due to a rise in sea level. It ultimately connected the Arctic Ocean with the Gulf of Mexico (Stanley, 1999). The seaway expanded and contracted several times during Cretaceous time. When it expanded and covered an area, dark-colored, fine-grained, and thin-bedded marine sediments were deposited, such as the Pierre shale that can be seen in outcrop between Las Vegas and Raton on Interstate 25. When the seaway contracted and retreated, beach, river and delta deposits built out and covered the marine deposits. The Dakota Sandstone consists of beach and river deposits (McGookey, 1972; Mateer, 1987). The seaway retreated forever from northeastern New Mexico at the end of the Cretaceous era. A new mountain range was rising nearby: the Rockies.

The Rocky Mountains make up what geologists call the Laramide orogeny, a period of mountain building and basin formation that began in late Cretaceous time and continued until the end of the Eocene epoch of the Tertiary period, about 34 m.y.b.p. The Rockies are a huge mountain belt, extending from Las Vegas and Santa Fe, New Mexico, into Canada. They are made up of a series of individual mountain ranges, with the one just west of Capulin Volcano and Raton called the Sangre de Cristos. Each range is bounded by large faults that accommodated the uplift of the mountains.

As the Sangre de Cristo Range rose, an area in the vicinity of Raton, called the Raton Basin, subsided. Rivers carrying debris from the mountains filled the basin and then continued east, depositing sediments across northeastern New Mexico. The rivers continued to do their work after the Sangre de Cristos stopped rising.

Those rivers were so plentiful and powerful that by late Eocene time the Rockies were much more subdued and worn-down than what we see today (e.g., Chapin and Kelly, 1997). What happened next, to create the modern Rockies, is the subject of intense scrutiny and debate by geologists. Some believe that the dramatic escarpment of the Sangre de Cristos and the Colorado Front Range has been created by renewed faulting and uplift (Steven et al., 1997). Others believe that the climate changed and the eastern slopes of these ranges were exhumed by powerful erosive forces (Chapin and Kelly, 1997). At least one author, working in the Sangre de Cristo, favors the faulting and uplift model (Dolliver, 1990). Either way, the dramatic Rocky Mountain front visible from Capulin Volcano was created just in the past five or so million years.

One of the most striking features of the RCVF is the dramatic height of Johnson and other mesas on the western edge of the field. They rise almost 1000 feet above the surrounding landscape. On the eastern edge, however, the mesas are on the order of just a few hundred feet in elevation (Stroud, 1997). This eastward sloping surface on which the lavas of the RCVF were extruded and which they now preserve mimics the general pattern of the Great Plains physiographic province.

The western mesas have only been exhumed over the last two or three million years, based on age determinations of the basaltic lava flows that cap them (Chapin and Kelly, 1997; Stroud, 1997). If this is the case for other parts of northeastern New

Mexico, it would indicate that the eastern front of the Rocky Mountains could be only one or two million years old.

The Ogallala Formation, deposited during the Miocene epoch, from 24 m.y. to 5.3 m.y., is a remnant of the apron of river sediment shed off the Sangre de Cristo range (as well as other ranges to the north and south—it covers a huge area). It covers a large portion of northeastern New Mexico, creating broad, flat areas and serving as a major source of ground water. The Ogallala and similar units form the Great Plains physiographic province in which Capulin Volcano lies. It is a relatively flat surface sloping from the mountains to the east, covering a substantial part of eastern Colorado, eastern New Mexico and other states to the east.

Volcanism in northern New Mexico

Eruptions in the RCVF began about 9 m.y.b.p. and continued until less than 60,000 years ago. Capulin erupted 60,000 years ago and thus represents one of the most recent eruptions. Baby Capulin lavas overlie those of Capulin, and are thus younger. Purvine Mesa and Twin Mountain are probably somewhat younger than Capulin also.

There has been widespread volcanism throughout the northern half of New Mexico. The two most voluminous geologic features related to volcanism in northern New Mexico are the Rio Grande rift and the Jemez lineament. The RCVF lies east of the rift and along the lineament. It represents the easternmost limit of late Cenozoic volcanism in New Mexico and western North America (Kudo, 1976) (Figure 1).

Figure 1a. Diagram showing the location of the Jemez Lineament, other major features in New Mexico and earthquake epicenters.

Source: http://krach.nmt.edu/R79/Figure2.gif

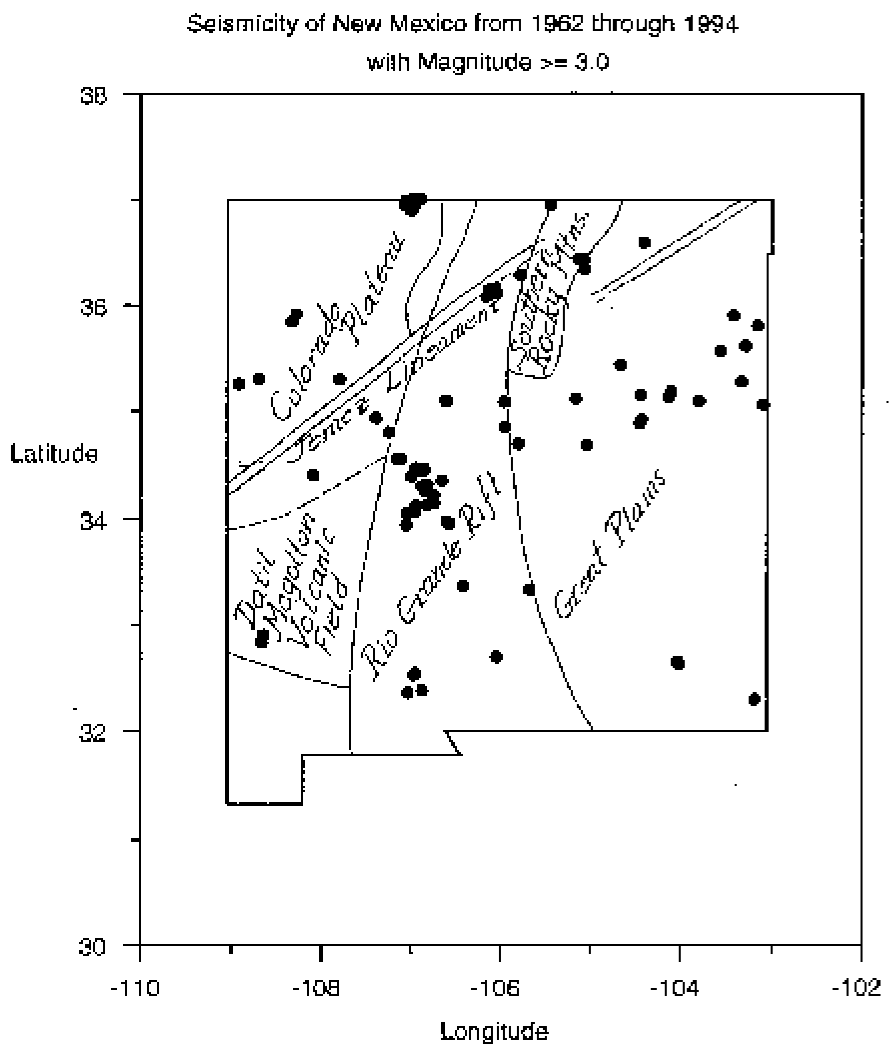

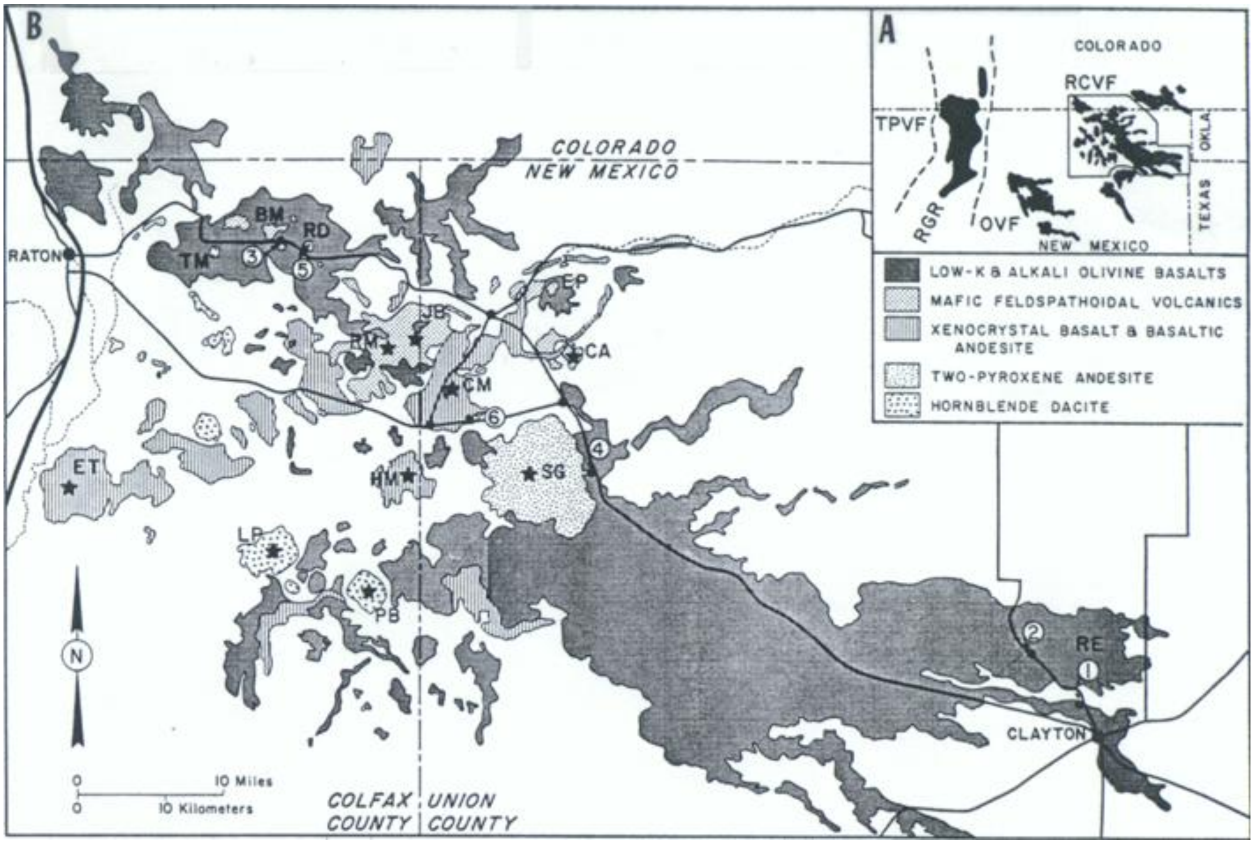

Figure 1b. Part A. Location of the Raton-Clayton volcanic field (RCVF), Ocate volcanic field (OVF), Taos Plateau volcanic field (TPVF) and Rio Grande rift. The outlined area is shown in part B. Part B. Distribution of volcanic rock types in the RCVF. The following volcanic features are shown: BM—Bellisle Mountain. CA—Carr Mountain. CM—Capulin Mountain. EP—Emery Peak. ET—Eagle Tail Mountain. HM—Horseshoe Mountain. JB—Jose Butte. LP—Laughlin Peak. PB—Palo Blanco. RE—Rabbit Ears Mountain. RD—Red Mountain. RM—Robinson Mountain. SG—Sierra Grande. TM—Towndrow Mountain. From Stormer, 1972.

Rio Grande Rift

The Rio Grande rift is one of only six continental rift systems in the world. A rift is an elongated trough bounded by large faults. It forms when the earth's continental crust starts to break along a roughly linear weakness and the two parts move away from each other. The Rio Grande rift is a north-south oriented zone extending from southern Colorado through central New Mexico and into Mexico. In northern New Mexico, it began to form about 26 m.y.b.p. (Dungan et al., 1989), and is still probably active.

A common misconception is that the Rio Grande cut the valley it lies in by itself. Rather, the rifting process created a broad trough that the river adopted as its own only about 3 m.y.b.p. Since that time, the river has cut several steep canyons (for instance, the Taos Gorge between the Colorado state line and Española), but the broader area between the mountain ranges is not due to river action.

Volcanism is often associated with rifting. Since the continental crust is stretched and thinned in this process, less pressure is on the underlying upper mantle and it rises up nearer the surface. With the decrease in pressure and the presence of hotter material nearer the surface of earth, melting takes place. The lavas originate from the upper part of the mantle, either within the lithospheric mantle (the uppermost part) or the underlying asthenospheric mantle. The two source regions produce lavas of different chemical make-up. By carrying out chemical analyses of the lavas, it is possible to reconstruct some information about their origin

The most prominent volcanic fields in northern New Mexico that are associated with the Rio Grande rift are the Jemez Volcanic Field and the Taos Plateau Volcanic Field (TPVF). The RCVF and the Ocate Volcanic Field, located southwest of the

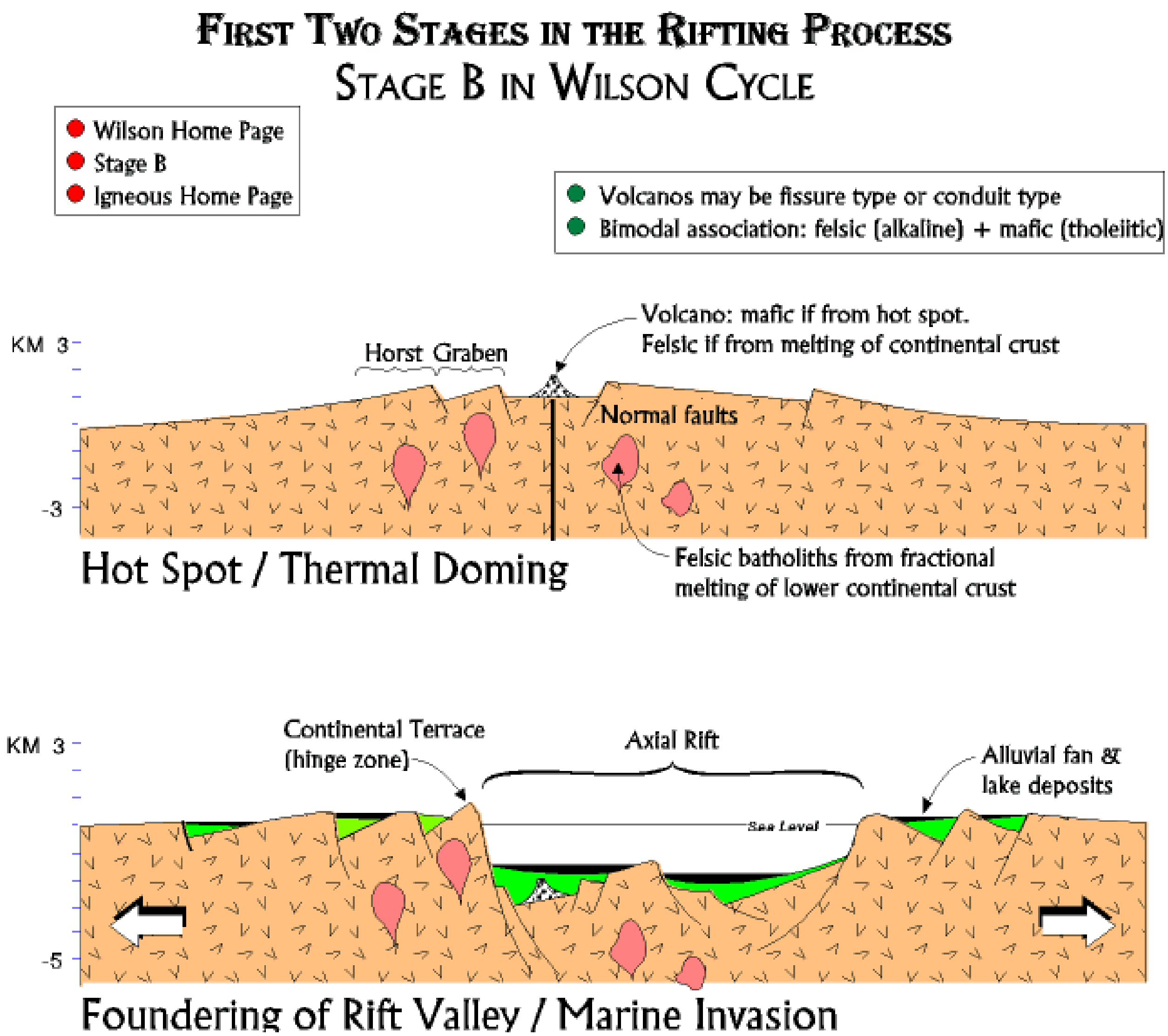

Figure 2. Diagrams showing the early creation of a continental rift. Rifting in New Mexico ended between the two stages.

Source: http://geollab.jmu.edu/Fichter/Wilson/Rift1-2.html

RCVF, are found to the east of the rift and share many chemical characteristics with the TPVF. All three volcanic fields were erupted over similar periods of time, and their lavas changed in their chemical make-up over time in a similar fashion (Dungan et al., 1989).

Jemez Lineament

The Jemez Lineament is a northeast-southwest alignment of late Cenozoic (about 6 m.y.b.p. to present) volcanic centers reaching from eastern Arizona to southeastern Colorado (Baldridge et al., 1984). The volcanic centers that lie along the Jemez Lineament (JL) are, from west to east, White Mountains and Springerville Volcanic Field of Arizona, and the Zuni-Bandera, Mt. Taylor, Jemez Mountains, Taos, Ocate, and Raton-Clayton volcanic fields of New Mexico. The JL crosses the Rio Grande rift in the vicinity of the Embudo fault system, which trends from southwest to northeast between Los Alamos and Taos. The Valles Caldera in the Jemez Mountains is at the intersection of the JL and the Rio Grande Rift. It may have contributed to the large magma flux.

There are several developed recreational sites in the volcanic fields of the Jemez Lineament: Sunrise Ski Resort in the White Mountains near Eagar, Arizona; El Malpais National Monument in the Zuni-Bandera field near Grants, New Mexico; Bandelier National Monument in the Jemez Mountains; Wild River National Recreation Site in the Taos volcanic field near Questa, New Mexico; and Capulin Volcano National Monument in the RCVF. The Wagon Mound, a distinctive butte used as a landmark by travelers on the Santa Fe Trail and above the town of Wagon Mound, NM, is in the Ocate volcanic field.

The Jemez Lineament is thought to be an old zone of weakness in the deeper crust that was reactivated again in late Cenozoic time, serving as a pathway for rising magmas from the upper mantle (Baldridge et al., 1984). The dominant trend of Proterozoic (2.5 billion years ago to 570 m.y.) faults is northeast, matching the JL. There is no clear age progression of volcanism from one end of the lineament to the other as would occur in a hotspot track. Also, its orientation does not match the orientations of individual volcanoes and smaller vents within the volcanic fields of northern and northeastern New Mexico (Dungan et al., 1989). Its origin and behavior remains an area of study for geologists.

In conclusion, the Rio Grande rift and Jemez lineament link together the volcanic fields of northern New Mexico and eastern Arizona. These fields are similar in age (late Cenozoic) and similar in chemistry, having been derived from the melting of the upper mantle and lower crust.

<u>History of the Raton-Clayton Volcanic Field</u>

The RCVF erupted in three phases: the Raton phase, Clayton phase and Capulin phase (Stroud, 1997, Baldwin and Muehlberger, 1959). The Raton phase lasted from 9.0 to 3.6 m.y.b.p., the Clayton stage from 3.0 to 2.2 m.y.b.p. and the Capulin from 1.7 to 0.05 m.y.b.p. The field is currently quiet. The Raton phase is generally found near Raton on the western side of the field, but also on the northern and southern perimeters (Figure 3). The Clayton phase is found on the eastern side of the field near Clayton, N.M. and scattered through the eastern half of the volcanic field, including Mud Hill near Capulin. The Capulin phase occurs in the general vicinity of Capulin volcano and the towns of Capulin and Folsom.

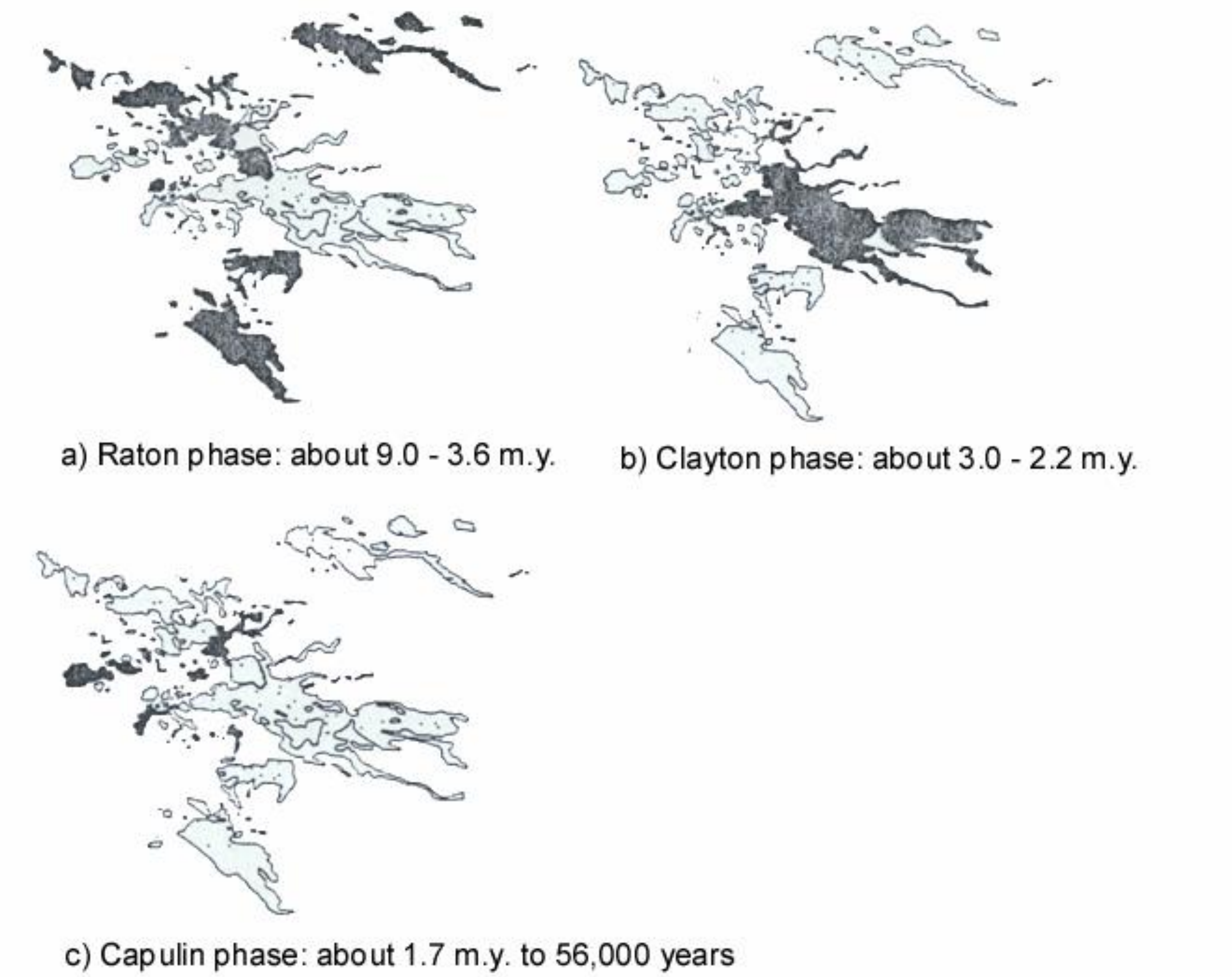

Figure 3. The location of Raton, Clayton and Capulin phases of the Raton-Clayton volcanic field (from Stroud, 1997).

The term basalt is used to describe the rock type found in greatest abundance in the Raton-Clayton, Taos and Ocate volcanic fields. Basalt is an extrusive igneous rock, formed by crystallization from molten rock flowing along the earth's surface (called lava), and made up chemically of low levels of silicon as compared to other rocks. Basalts typically have 48-53% silicon dioxide, while andesites, such as those of Sierra Grande, range from 53 to 63% silicon dioxide. Dacites and rhyolites, such as those common in the Jemez Mountains and found at Red Mountain in the RCVF, range up to 77% silicon dioxide.

The Raton phase of lavas can be further subdivided into several groups. One group is a type of basalt called alkali olivine basalt or alkali basalt (Dungan et al., 1989). This type of basalt is commonly associated with continental rift systems (Hyndman, 1985), although it is puzzling that it is not found in the Taos volcanic field, but only in the Raton-Clayton and Ocate fields (Dungan et al., 1989). These basalts were derived from melting within the mantle at about 100 kilometers below the surface.

The other important group of rocks within the Raton phase is the Red Mountain rhyodacite (Stroud, 1997). These rocks were erupted between 6.8 and 6.3 m.y.b.p. (Stroud, 1997). Rhyodacite looks very different from basalt, primarily being lighter in color. It makes up Red Mountain on Johnson Mesa to the northwest of Capulin Volcano, and several other volcanic centers in the area. The different color is due to a much higher concentration of silicon and oxygen. This different chemical composition is due to two major processes: melting of the lower crust triggered by the injection of basaltic magma from the upper mantle and a process called crystal fractionation, in which dense crystals form in a magma and settle out, leaving behind a magma depleted in the elements contained in the crystals (Dungan et al., 1989). For example, because olivine crystals that settle out are rich in magnesium and iron and poor in silica, the magma left behind is poor in magnesium and iron and enriched in silica. Similar processes take out many elements and concentrate others, and the composition evolves toward a rhyolite.

The Clayton phase is made up of two rock types called nephelinite and basanite. The rocks look like basalt when viewed in outcrop, but they contain extremely low (42-45%) amounts of silicon dioxide (Stroud, 1997, Dungan et al., 1989). Eruption of Clayton phase lavas began around 3.0 m.y. at Rabbit Ears, an eroded vent near Clayton, visible from the Capulin rim trail. Most of this stage of volcanism in the RCVF is found between Clayton and Sierra Grande. However, Jose and Robinson buttes, west of Capulin volcano, are Clayton age. Stroud (1997) did not determine the exact age of these cinder cones, but they were probably erupted late in the Clayton stage, at around 2.5 m.y.b.p.

An important rock type that was erupted during both the Raton and Clayton phase of volcanism is the Sierra Grande andesite (Stroud, 1997). The most prominent feature formed by these rocks is Sierra Grande itself, the largest volcano in the RCVF. It erupted between 3.8 and 2.6 m.y.b.p. (Stroud, 1997).

The Capulin phase of the RCVF began about 1.7 m.y.b.p. and continued until a few thousand years after the eruption of Capulin volcano (Stroud, 1997). There is no evidence to suggest that it has ended, and so may simply be in an eruptive hiatus. These lava flows are basalt and were derived from the melting of the mantle, although many lavas contain quartz crystals derived from the disaggregation of chunks of crustal rocks that were incorporated into the ascending magma. Capulin flows are located in the central and western portions of the RCVF.

Body of Report

Study area

Our research was limited to the National Monument and those ranches that we had access to, primarily the Morrow Ranch, and most of Sierra Grande. For other areas, aerial photography taken by other federal agencies allowed for the development of a geologic map of all of Capulin's flows. The area within the boundaries of the Monument was studied in greatest detail. Mud Hill was investigated because of its distinct eruptive character, and Baby Capulin was studied because of its similarities to, but younger age than, Capulin. Sierra Grande was the subject of a master's thesis by a student at Northern Arizona University, Jerome Hesse, under the direction of Dr. Ort, with the goal of understanding how so much andesite was erupted in one place and nowhere else in the RCVF.

Methods

The major goal of mapping was to identify all mappable volcanic features that would contribute to an understanding of the eruption history. Field mapping required us to be able to identify rock types and lava flow features while at the same time being able to locate ourselves on a map accurately. Geochemical analyses on fresh, unweathered specimens were carried out at Washington State University. Major and some trace elements were analyzed by x-ray fluorescence (XRF), while other trace elements were analyzed using an inductively coupled plasma mass spectrometer (ICP-MS). Information on the analytical processes is provided in Appendix I so that subsequent workers can determine how the chemical data were obtained, and therefore how they might be compared to other data.

Paleomagnetic sampling was done with a portable rock drill. Samples were taken from fresh, unfractured portions of outcrops and oriented with a sun compass where possible, as magnetism in the outcrops affected the compass in some locations. Dr. Ort did laboratory analysis at University of California, Santa Barbara, on a Molspin spinner magnetometer using AF demagnetization.

We attempted to determine the age of volcanism using paleomagnetic techniques. All rocks are magnetic, and basalt is particularly so, due to the abundance of the mineral magnetite. As the basalt cools and solidifies, the magnetite's magnetic field aligns with the earth's magnetic field. This magnetism is "frozen" in the rock, and it is possible to retrieve it. The rock must be "cleaned" magnetically to remove the presence of younger, spurious magnetic directions. Dr. Ort carried this out at the University of California, Santa Barbara. In studies of rocks as young as Capulin's, the direction is then compared to magnetic directions from lake sediments and rapidly extruded volcanic rocks whose ages are known. Theoretically, there is enough variation in magnetization in those records to match Capulin's magnetization to an identical magnetization of known age. However, we determined that the magnetization revealed in the cleaning process was not anywhere close to the directions of the magnetic field at about the time we suspected Capulin was formed. The data also had a large amount of variation within the sites, suggesting that the rocks did not have a stable magnetization. We also determined that the original magnetization of rocks sampled near the rim of the volcano had been destroyed by lightning strikes. Paleomagnetic data are not included in the Appendices because they are voluminous and inconclusive. Joseph Stroud originally intended to use paleomagnetism in his thesis work, but also found that the magnetic remanence was unstable.

The cosmogenic helium age determination is a method of determining how long a surface has been exposed to the atmosphere (Cerling, 1990). Cosmic rays and muons produced by the sun and other stars enter earth's atmosphere and travel through it. Some of the rays are slowed and stopped, due to interaction with the atmosphere, but most make it to Earth's surface. These cosmic rays penetrate centimeters to decimeters into a rock, spall (break) heavier atoms in the rock and split them into smaller atoms, especially helium-3 (^{3}He). The cosmic ray flux is relatively constant, and its small variations have been documented in detail. Therefore, the production of ^{3}He, normally a very scarce isotope, occurs at a steady, known rate at earth's surface. The ^{3}He:^{4}He ratio, which compares the amount of cosmogenic helium (^{3}He formed by cosmic ray bombardment) with normal helium (^{4}He, common in the atmosphere and rocks), is then used to determine the amount of time a rock surface has been exposed to the atmosphere. A correction is made for altitude and latitude to account for the effects of the atmosphere on cosmic rays. The corrections that were used for this date are included in Appendix II.

Careful sampling is required to determine the age of an eruption using cosmogenic methods. A sample must be found that has been at the surface in its present orientation since cooling and has not been shielded from cosmic ray bombardment by vegetation or steep slopes. At Capulin, we sampled a squeeze-up in the *boca* where lava squeezed upward through a crack in the roof of a lava tube, creating a thin spine. This feature has remained in this form, with scrape marks on its side, since the lava flow cooled. It also has a large field of lava rubble around it, with no trees or vegetation to shield it from cosmic rays, and it is not in a position for deep snow to build up. These circumstances lead us to interpret the cosmogenic helium date as the age of the lava flow sample. The date came from an olivine separate from the sample.

The radiocarbon method for determining the age of carbonized logs or underlying soils in order to date the associated lavas has been used successfully in other studies. The technique requires that organic material be found that was alive at the time of eruption. We had hoped to use this method, but we never found any organic material preserved as charcoal in a tree trunk mold or carbonized soil under a flow. Our new He date indicates that any carbon would be too old for the ^{14}C method.

Results

1. Capulin volcano is about 60,000 years old, based on our cosmogenic helium date and on the $^{40}Ar/^{39}Ar$ dating by Joseph Stroud (Stroud, 1997).
2. The earliest flows issued from the east side of the volcano. The next oldest flows were emplaced south, then west, and the youngest are to the north. The largest amount of lava produced by the volcano came from the west side and formed the *boca* or mouth of the volcano, which includes several vents, tubes, lava lakes, lava cascades and levees.
3. Mud Hill erupted more explosively than Capulin, producing some lava but more pyroclastic (fragmental) material. It is older than Capulin.
4. Baby Capulin erupted in a similar style to Capulin. It is younger than Capulin.

5. Geochemical analyses determined that the lavas at the volcano originated in the mantle, but an accurate analysis was made difficult by the presence of quartz grain contamination from the rocks underlying the volcano through which the magma traveled before reaching the surface, chiefly the Dakota formation.

Assistance given the park in improving and expanding public interpretation programs

1. In 1996, Dr. Ort assisted the park in the creation of a new geologic map for the park brochure.
2. In 1995, the park staff assembled an interpretive display on our work.
3. During each field season, Student Conservation Association volunteers, NPS volunteers and park staff accompanied us in the field to learn more about our work.
4. In 1996, Dr. Ort provided input on the written part of a new display at the visitor center.
5. We have suggested that a new interpretive trail be constructed in the *boca*.
6. In 1997, we made a video (Dr. Ort narrated and Dr. Sayre operated the camera) of the park and surrounding areas reviewing our work.
7. In a somewhat unrelated field of study, Dr. Sayre has suggested the park develop a new interpretive direction in meteorology. Capulin has more thunderstorm days than anywhere does in the U.S. outside of the Gulf Coast (Nese and Grenci, 1998).

Input given the park in natural resource management issues

1. In 1993 and 1994, Dr. Sayre provided technical input to the park in its boundary study. This included speaking at public events and discussing issues with NPS staff at the park and at regional headquarters.
2. In 1998, Dr. Sayre made presentations about this project at public meetings at the park as part of the preparation of a General Management Plan.

Assistance given the park in recognizing and mitigating potential threats

1. Dr. Ort has determined that the thickness of the cinder deposits on the older flows decreases as distance from the volcano increases. Cinder mining will, therefore, be most likely closest to the volcano.
2. We have had general discussions with park staff about the arroyo formation on the flanks of the volcano and rock falls on the road, but we have not made any specific recommendations.

Discussion and Conclusions

The age of Capulin Volcano

Previous studies had attempted to estimate the age of the Capulin flows by correlation with the Folsom Man site. Sayre et al. (1995) describe the arguments involved in this. Here, we report the best dates we have for the eruption of Capulin volcano.

In conjunction with Dr. Mary Reid of University of California, Los Angeles, and Dr. David Graham of Oregon State University, we made a cosmogenic helium exposure date on a lava squeeze-up in the northern *boca* (appendix II). This type of date measures how long the rock has been exposed to bombardment by cosmic rays and muons. The best date is 62,000 years before present, with a potential error of 10% or about 6,000 years (Sayre et al., 1995).

Joseph Stroud, a masters student at New Mexico Institute of Science and Technology under the direction of Dr. William McIntosh, made several $^{40}Ar/^{39}Ar$ dates of lavas of Capulin volcano (Stroud, 1997). This is an isotopic age determination based on the decay of naturally occurring radionuclides. His best date for Capulin, averaged over four different samples, is 58,000 years before present, with an analytical error of 4,000 years. This type of date measures when the lava cooled, rather than how long it has been exposed. It is difficult to date a basaltic rock this young because the amount of radiogenic argon is quite low, so Stroud was required to date several samples.

The two dates, determined by different methods, agree within analytical errors. This leads us to trust their validity and suggests that Capulin is about 60,000 years old, with an approximate analytical error of 4,000 years.

The geomorphology, or shape, of Capulin volcano also indicates that it is not particularly young, although such an analysis cannot determine an absolute age. Cinder beds at the outer edge of the rim of the volcano dip inward toward the crater. If a volcano were young and little affected by erosion, we would expect outward-dipping layers. As a volcano ages, outward-dipping cinder beds on its rim are likely to be removed by erosion, leaving only the inward dipping portions.

More geomorphic evidence relates to a prominent 30-foot-thick spatter flow located on the southeastern edge of the rim, visible from the road between Folsom and Des Moines. A spatter flow resembles a normal basalt flow; however, it is formed by the agglomeration of small amounts of lava (spatter) thrown out of a vent and extends for only a short distance. The Capulin spatter flow is partially unsupported by cinder deposits and juts out approximately 30 feet from the side of the volcano. If the volcano were young, we would expect the flow to be completely surrounded by cinder. In an older volcano, we would expect erosion to carry away some of the cinder, leaving the spatter flow exposed.

Finally, loose cinders form an apron around the volcano, indicating that they have had time to erode from the main cone, even though erosion is slow in this dry climate. This line of reasoning also indicates that the volcano is not particularly young.

The eruption of Capulin Volcano

The Capulin eruption probably began with a fissure vent oriented in an ENE-WSW orientation, with the final Capulin cinder cone and *boca* located along it (Figure 4). This fissure eruption likely did not last long. Evidence for this phase of the eruption is scarce, but its existence is inferred from a lineation of early, small vents. These include the small vent near the cinder pit on the northeast side of Capulin cone, the main vent of Capulin cone, and a small vent about two hundred meters north of the picnic area (Figure 4). These small vents are interpreted to represent the localization of the fissure into several small vents. It is also possible that the Capulin eruption began with a lineation of several small distinct vents. However, it is common for basaltic eruptions to begin with fissure vents, as magma tends to move in tabular bodies (dikes) perpendicular to earth's surface, rather than as pipes, so we prefer the fissure interpretation, with subsequent localization of the eruption into several discrete vents.

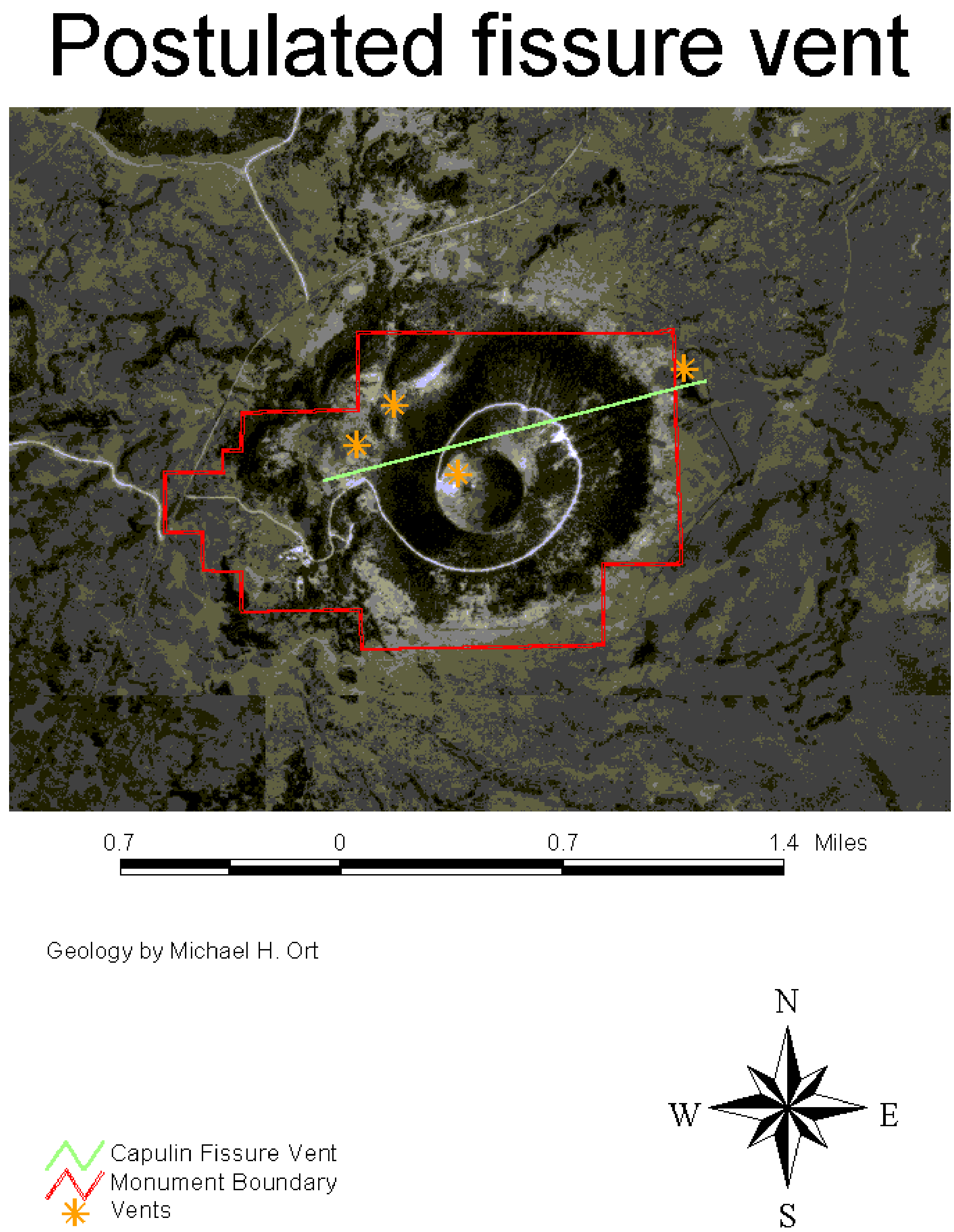

Figure 4. Capulin's first eruption, along a postulated ENE-WSW fissure.

A moderate-sized lava flow is interpreted to underlie the cinders to the east of the cinder cone, and likely formed from fountaining from the fissure vent or few small vents early in the eruption (Figure 5). Evidence for this is:

- The large plateau with subdued flow surface features that stretches out from the cinder cone. This is covered by cinders from Capulin, so must have been emplaced early in the eruption, or pre-eruption.
- In the cinder pit to the southeast of Capulin cone, an intricate mingling of lava with cinders is seen. This suggests that the lava was flowing at the same time the cinders were falling on its surface.

Later, the vents coalesced into one main vent, the cinder cone. The cinder cone eruption occurred for a period of weeks to years. The prevailing wind blew from the west, depositing more cinders to the east than to the west. This also helped make an uneven crater rim that is higher on the east, an asymmetry that is still preserved. Cinders fountained high into the air, perhaps as high as 500 m, during the eruption, and the cinders fell back to Earth around the vent, leading to the formation of a pile of cinders. These cinders built up to the angle of repose, the maximum slope angle at which the cinders were stable. When it exceeded this angle, the cinders would avalanche down the mountainside, leading to the formation of a layered deposit. The cinder cone eruption ceased when the magmatic gases started becoming less abundant, which resulted in less pressure to send the lava flying into the sky. As the eruptive column decreased in height, cinders changed to spatter (larger pieces, being heavier and with less gas pressure behind them leading to less airtime for cooling), forming the spatter rampart that protects the rim and coats the inside of the cone. In

Figure 5. The moderate sized flow to the east, under cinders. A dark line outlines the outer edge of the flow.

eruptions of higher silica magmas (which are more viscous), the magmatic gases themselves break the magma into pieces, forming pumice, and providing a great deal of explosive force to the eruption. In basaltic eruptions like this one, the magmatic gases provide some force to help send the lava skyward, but breaking of the lava into cinders tends to happen passively in the air. Spatter commonly comes from gas bubble bursts through a magma body, such as a lava lake in the vent, and coats the entire inside of the crater.

The main lava flows started after the cinder cone eruption had ceased. Their appearance after the cessation of cinder cone activity is indicated by the lack of cinders on top of the flows. The flows came out of the *boca*. This may be because the cone was lower on that side, due to the prevailing winds, so there was less weight to hold the lava back. The lava oozed out of the side of the cinder cone (the area is visible where the lavas of the *boca* buttress against the edifice, Figure 6), and probably carried some cinders with it. This undermining may have further lowered the west rim of the cone.

The early flows went down to the south (Figure 7), traveling down the narrow valley through what is now the picnic area. The spatter from these flows can be seen on the western ridge of this small defile (Figure 8). Fairly soon after the lava started to flow, its upper surface cooled to form a rocky cover, insulating the lava from further cooling. Thus, a lava tube formed. These flows traveled south and then spread eastward, following the local topography. Tumuli, blisters of lava which produce small conical hills, formed on flat areas below the steeper slopes, where pressure from within the lava flow forced lava out through cracks (Figure 9). The large push up/squeeze up feature in the picnic area (Figure 10) came from a pressure increase, possibly due to a

Figure 6. The earliest vent, indicated by white arrow.

Flow Series and Vents

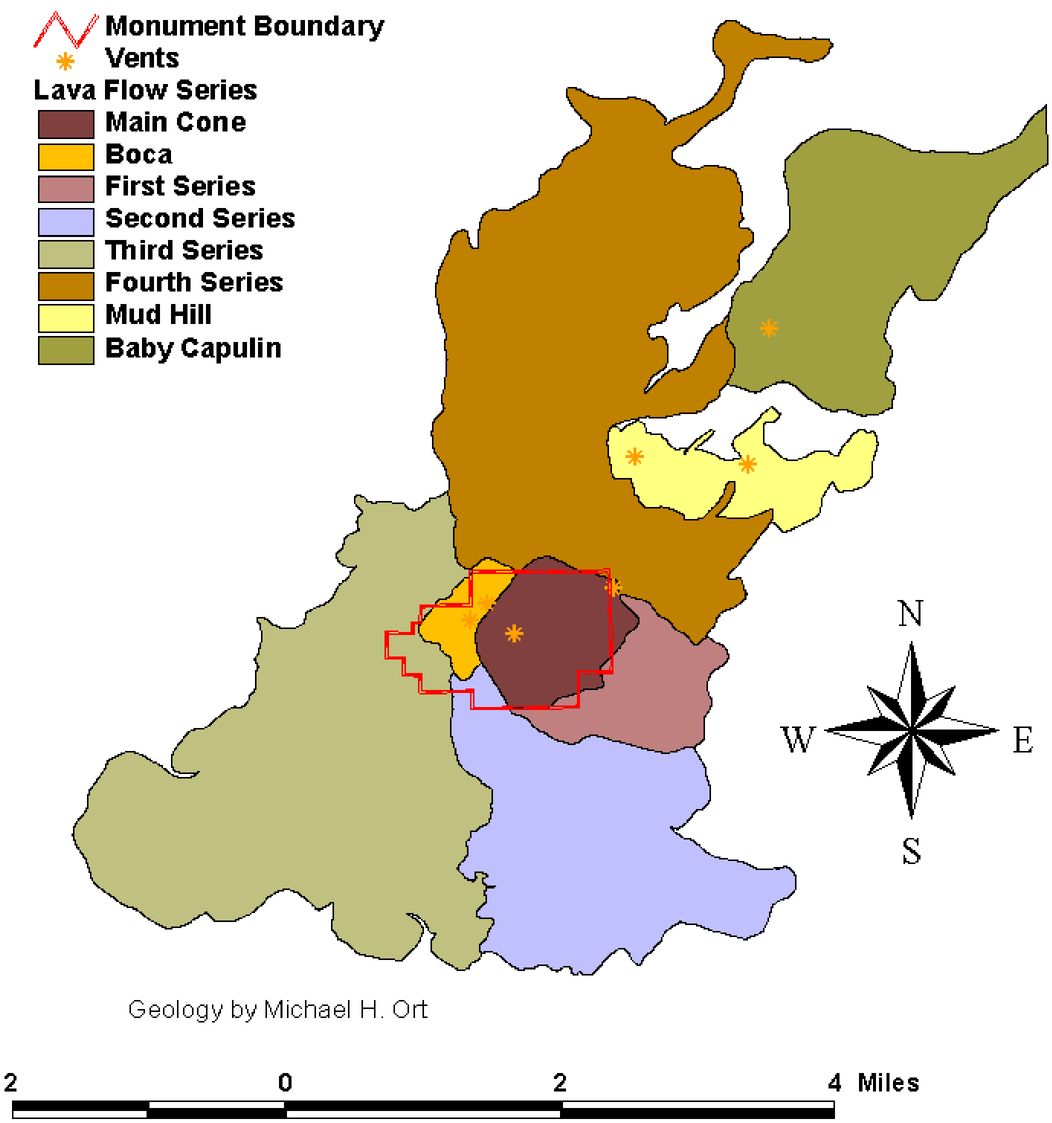

Figure 7a. Lava flow series of Capulin Volcano

Figure 7b.   Southern flow series. View to south.

Figure 7c. Southern flow series. View to southeast with Sierra Grande on horizon.

Figure 7d. Southern flow series. Close-up of compressional flow ridges.

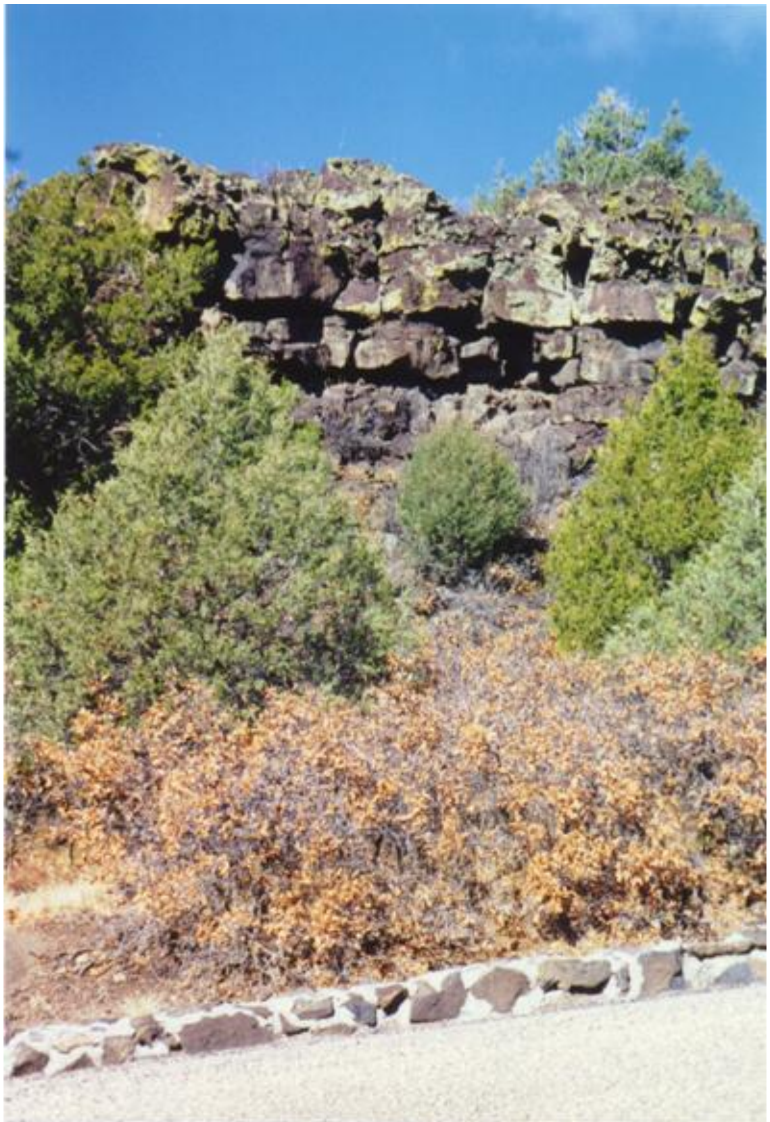

Figure 8. Outcrop on western edge of road near picnic area, showing spatter layers.

Figure 9. Tumulus on nature trail next to visitor center.

Figure 10. Push up (left) and squeeze up (right) at picnic area.

blockage downstream, which caused a part of the roof of the lava tube to be pushed out. The rest of the tube evidently collapsed and was carried away. This phase of the eruption ended when a chunk of the cinder cone was pushed out by the lava, blocking egress along its previous route. This piece of cinder cone is visible as the hill northwest of the hairpin turn near the picnic area (Figure 11). It is made of cinders and spatter.

At this point, the presently visible lava lake system of the *boca* began to develop, fed by a vent located at the southern edge of the *boca* (just over the first rise when one is walking up from the picnic area) (Figure 12). This vent area is marked by spatter ramparts, and spatter on the side of the cinder cone. A small alcove in the rampart has been called a "cave" by some. The first lavas continued southward, but now with a westward component (Figure 13). These lavas formed a pair of lakes near the old campfire chimney in the *boca* (Figure 14), then traveled by tubes (now visible as elongate holes filed with large lava rubble) (Figure 15) down to the area of the visitor's center plateau, where tumuli formed. From there, they traveled via tubes and open flows down toward what is now the town of Capulin, and to the west. The lakes themselves were bounded by walls made of spatter and by "bulldozed" solid lava from the edges of the flows. As time went by, these lakes were cut off from the vent, perhaps when there was a brief eruptive hiatus.

Next, a lava lake formed directly on the west side of the *boca* (Figure 16), fed by a new vent just north of the previous vent (Figure 17). This vent is on the other side of a tall spatter rampart (Figure 18), and the lava flowed into a lake north of the previous ones. This lava again flowed out of the *boca* region via tubes, and flowed toward the

Figure 11. Hill formed by magma pushing out the side of the cinder cone.

Figure 12a. First major vent in *boca* viewed from rim trail. Vent is shaded depression just below center of photograph.

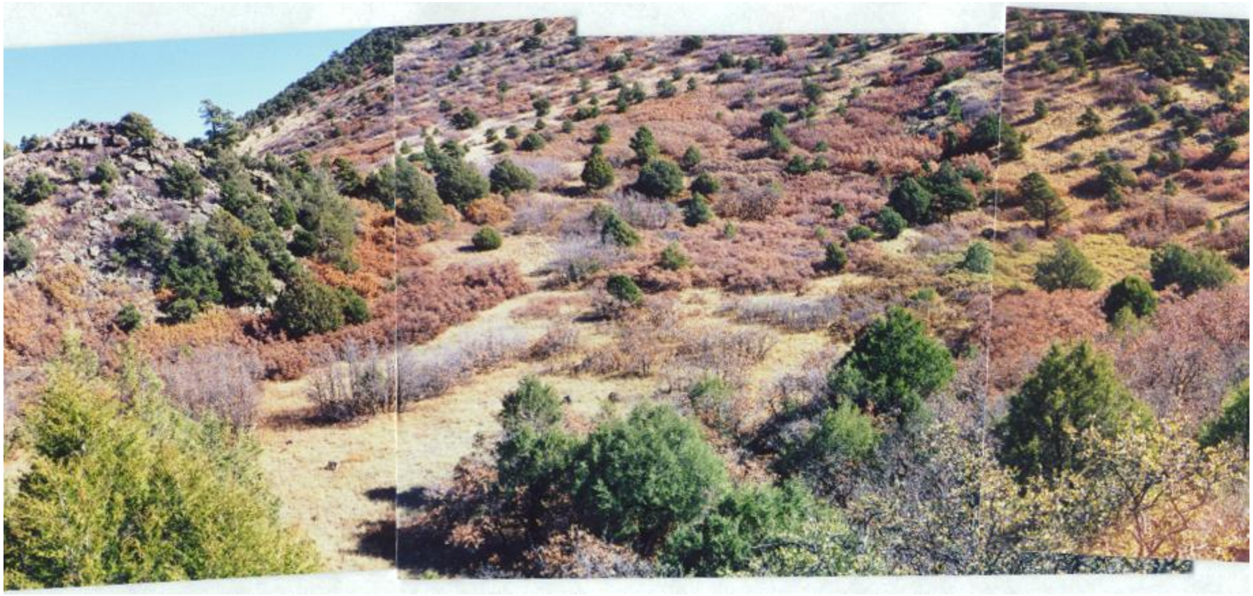

Figure 12b. First major vent in *boca* viewed from ground level.

Figure 13. Southwestern lava flows.

Figure 14. Lava lake near the campfire chimney. Lake is flat, grassy area in middle distance.

Figure 15. Lava tubes leading from campfire chimney.

Figure 16. Second lava lake north of the first two, west of the vent in Figure 12.

Figure 17. Second major vent in *boca*, north of first major vent.

Figure 18a. Spatter hill between first and second major vents. It is the dark hill in the middle distance.

Figure 18b. Spatter hill between first and second major vents, from rim trail.

west along a pre-existing drainage divide, and thence to the south. Tubes and tumuli are visible below the *boca's* ramparts (Figure 19).

Eventually, this lake began to drain to the north, through a now collapsed tube clearly visible in the north *boca* region (Figure 20). The tube fed a northern lake within the *boca* (Figure 21), at the lowest elevation of any of the lakes. This tube drained north of the drainage divide, thus sending future flows to the north. The northern lake, in turn, fed the flows that traveled to the north, some as far as Folsom (Figure 22). This part of the eruption ceased when a large piece of the cinder cone was rafted out about 100 meters, forming a ridge at the northern end of the *boca* that is clearly visible from the highway when one is traveling southward (Figure 23). Lavas now came from the northeasternmost edge of the *boca* and flowed in the region between Capulin and Mud Hill and to the east on top of Mud Hill deposits (Figure 24). The eruption then ceased. The lava flows cover about 41 km^2 (15.7 square miles). Their average thickness is not known nor knowable without extensive trenching, so any estimate of their volume is very imprecise. If an average thickness of 5 m is assumed, the total lava flow volume is about 0.2 km^3 (0.08 cubic miles). The cinder cone is approximately 0.4 km^3 (0.09 cubic miles). An unknown, although probably much lesser, amount of cinders is spread across the terrain to the east of the volcano. A total volume of about 0.6 km^3 is a moderate-sized cinder cone and lava flow eruption.

The Capulin and Baby Capulin basalts are actually trachybasalts, which means they have more abundant alkali elements than are present in true basalts. They contain scarce olivine and plagioclase phenocrysts (crystals that formed from the magma itself), as well as quartz and sodic plagioclase (distinct in appearance and

Figure 19. Lava tubes leading to the west from the *boca*. White arrows indicate tubes. Small tree-covered tumuli dot the plains surrounding the tubes.

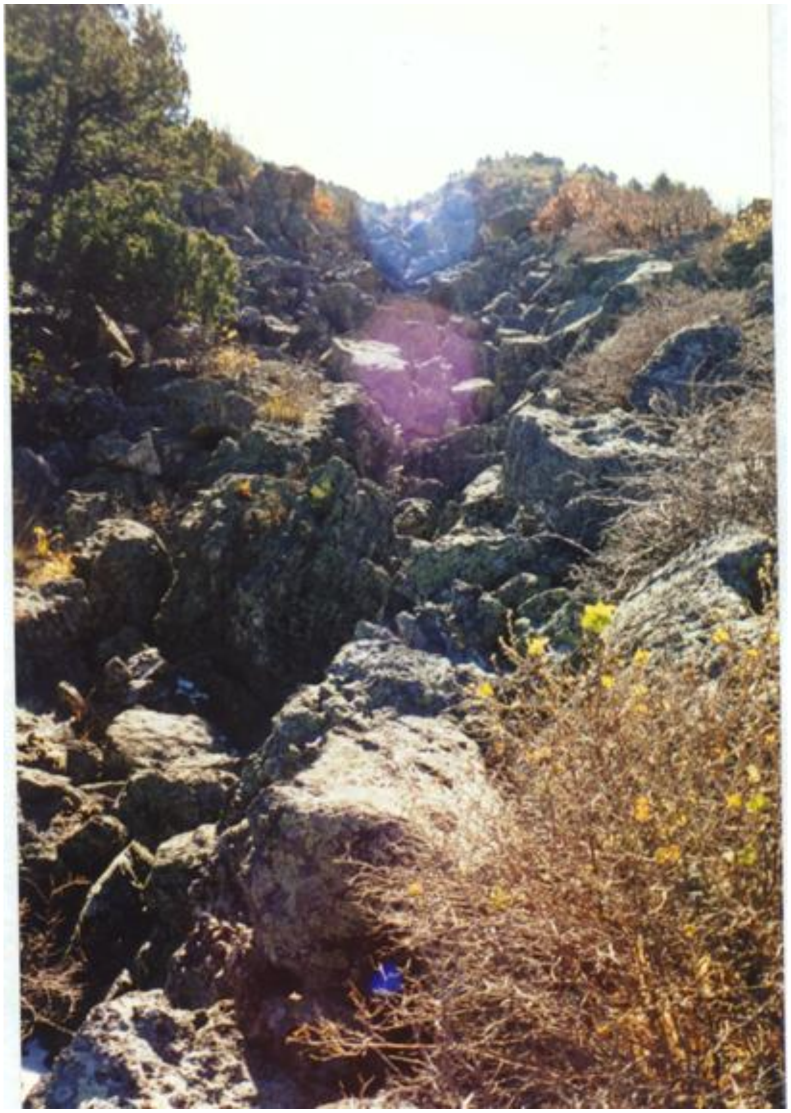

Figure 20. Collapsed tube leading north from second major vent to youngest lava lake.

Figure 21. Northernmost, youngest and lowest lava lake.

Figure 22. Northern flows.

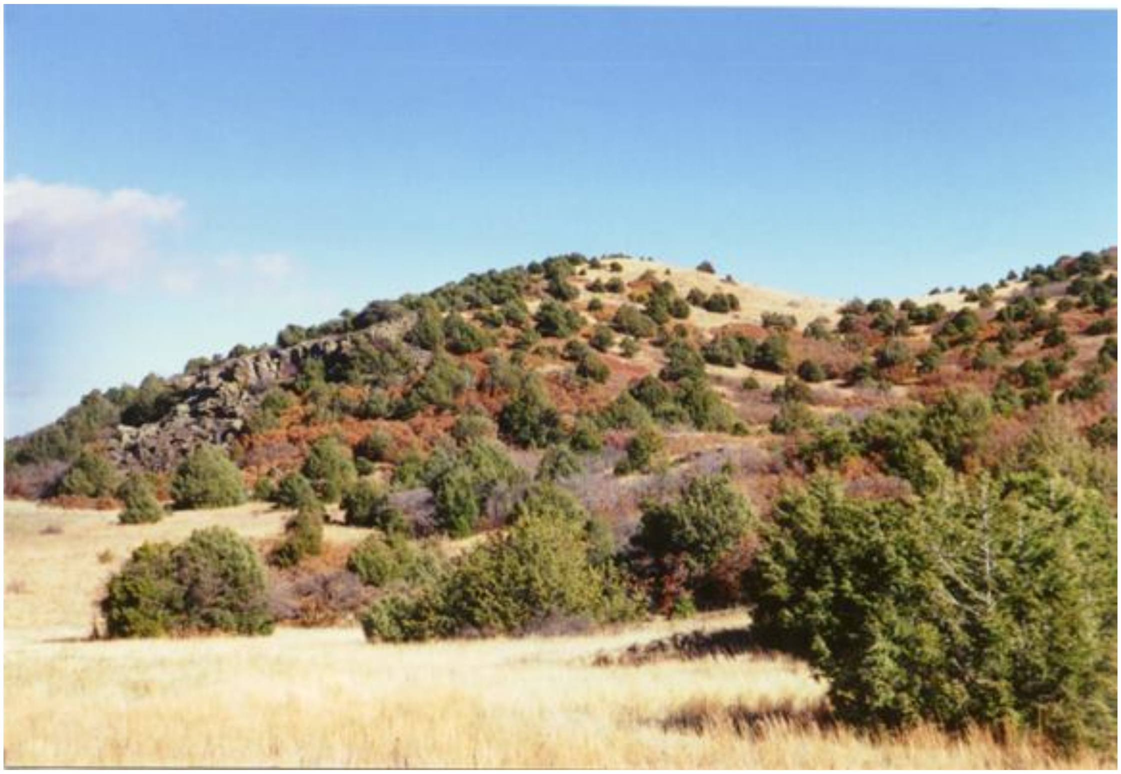

Figure 23. Large portion of cinder cone on northwest side of *boca* pushed out by magma late in the eruption.

Figure 24. Flows between Capulin and Mud Hill.

composition from the phenocrystic plagioclase) xenocrysts (crystals that contaminate the magma), in a groundmass of plagioclase microlites and glass. The xenocrysts have resorbed edges, giving them a rounded shape, and the sodic plagioclase crystals have fritted, resorbed cores with more calcic rims.

The eruption of Mud Hill

The Mud Hill volcano formed by a very different process from Capulin volcano. Mud Hill was considerably more explosive, due to gases formed from heating groundwater. In this kind of eruption, called a phreatomagmatic eruption, the groundwater flashes to steam, expanding tremendously, and explodes. When this occurs, the magma is broken into pieces. These pieces are called ash (< 2 mm in diameter), lapilli (2 – 64 mm in diameter) and blocks and bombs (> 64 mm in diameter, with blocks being hardened pieces of lava and bombs being liquid lava at the time of ejection from the vent). These are collectively known as pyroclasts. They are spread out over the land by laterally moving currents (called surges), fallout (pyroclasts falling out of the eruption plume) and ballistic trajectories (thrown from the vent and forming an arc as they fly through the air to their landing). The resulting crater, which commonly (although not at Mud Hill) fills with water, is called a maar volcano, and Mud Hill is of the particular type called a tuff cone.

The eruption began with an east-west oriented fissure eruption. This is clearly visible from the Crater Rim trail at Capulin as a series of low hills extending eastward from Mud Hill (Figure 25). Volcanism along this fissure quickly settled down to a couple of vents, including Mud Hill and vents to the east that produced lava flows that extend to the north of them. The vents themselves show spatter oriented parallel to the fissure.

Figure 25. Mud Hill. Mud hill fissure vent outlined by white line.

After a period of time, probably hours, the eruption focused on the Mud Hill vent. It probably did this because the magma had heated the groundwater above boiling. This magma/water interaction led to great explosions that left a low crater with rims made of pyroclasts. These pyroclasts, being of ash, lapilli, and block sizes, form a phreatomagmatic tuff. The rims gradually grew taller, until another major explosion, slightly off center from the previous explosions, carved out a new vent area, and then began forming another cone. Beds from this new cone are at a high angle to the previous beds, and can be seen on the north side of the volcano. This cone grew to the present height.

At this point, most groundwater in the area had been used up in the explosions, and lava began to pour into the crater. Eventually, it broke through to the south, carrying off part of the cone and forming a long lava flow to the east of Mud Hill. The eruption then ceased. Lavas from Capulin have subsequently altered the area to the south of Mud Hill.

Mud Hill lavas contain olivine phenocrysts in a groundmass of plagioclase laths, with some tiny crystals of pyroxene, olivine, and opaque oxides.

The eruption of Baby Capulin

Baby Capulin is younger than Capulin volcano. We observed, on aerial photographs, a Baby Capulin flow that flowed out upon a Capulin flow. It formed from a cinder cone-forming eruption that produced more lava flows than it did cinders. At least one of these flows, visible from the road from Capulin to Folsom, overlies a Capulin flow, indicating that Baby Capulin is younger than Capulin. The present cinder cone formed early in the eruption, along with a number of spatter cones that surround the cone to the south and east (Figure 26). These spatter cones fed the lava flows that

Figure 26. Baby Capulin, indicated by arrow.

traveled northward to Folsom and into the Dry Cimarron valley. These are likely the same flows present at Folsom Falls and farther downstream. Due to access problems, we were not allowed to map the entire Baby Capulin area. Baby Capulin lavas are similar in petrographic appearance to Capulin lavas, except that they contain fewer xenocrysts.

The eruptions of Sierra Grande

Sierra Grande is the largest volcanic edifice in the Raton-Clayton volcanic field. It consists almost entirely of andesitic lavas, a more silica-rich lava than basalts. This makes the lavas more viscous than basalts, and produces thicker lava flows that form steeper slopes. Although it has been called a shield volcano, this is incorrect, as the slope angles are too great. It is a stratovolcano predominantly composed of andesite lavas. Stratovolcanoes are typically composed of layers of lava flows and volcaniclastic deposits, but in dry environments volcaniclastic deposits are commonly rare and typically are represented only in the flat lands around the base of the volcano. The eruptions of Sierra Grande probably took place over a period of hundreds of thousands of years, making it a much longer-lived volcano than Capulin. The ascent of magma beneath it was probably controlled by structures deep in the earth. In some locations, low-K basalt flows occur with structures indicating flow from beneath the Sierra Grande edifice, and presumably earlier in time. We interpret this to indicate that the center produced voluminous basalt flows prior to the construction of the stratovolcano. Sierra Grande erupted andesite lavas while constructing the main volcanic edifice. Vents were both at the present summit and as satellite vents along the sides of the volcano. Some of the late eruptions were of a magma type called nephelinite, which is very low in silica. These vents are on the lower sides of the volcano.

Sierra Grande is composed of about 23 km^3 of fairly compositionally homogeneous, phenocryst-poor olivine-clinopyroxene mugearites and two-pyroxene benmoreites. Three mafic feldspathoid-bearing cinder cones are exposed on and near the flanks of Sierra Grande. Orthopyroxene phenocrysts are reverse-zoned with iron-rich cores (Wo_2, En_{68-77}, Fs_{21-29}) and magnesian rims (Wo_{2-4}, En_{77-84}, Fs_{14-20}). Their rims are in equilibrium with the surrounding magma with respect to partitioning of iron and magnesium. Olivine compositions and orthopyroxene core compositions are in disequilibrium with the surrounding magma. Two-pyroxene geothermometry produced equilibrium temperatures from 1010$\pm$60 to 1125$\pm$60 ^{o}C. Rare earth element and high field strength element concentrations decrease with increasing differentiation. $^{87}Sr/^{86}Sr$ values (0.7043-0.7047) approximate bulk earth values. Pb isotope ($^{206}Pb/^{204}Pb$ = 17.58 - 18.08; $^{207}Pb/^{204}Pb$ = 15.46 - 15.51; $^{208}Pb/^{204}Pb$ = 37.30 - 37.80) and ε_{Nd} (-3.6 to -1.2) values are the lowest in the RCVF and indicate a lower crustal component. Three important features, 1) disequilibrium phenocrysts, 2) decreasing REE concentrations with increasing differentiation, and 3) isotopic values indicative of a lower crustal component, are best explained by magma mixing between a mantle-derived magma and a lower crustal melt. Isotopic modeling shows that as much as 30% lower crustal melt mixed with alkali olivine basalt to produce the bulk of the Sierra Grande lavas, and an upper crustal component is present in the most mafic Sierra Grande sample. As mantle melting waned, eruptions from Sierra Grande ceased, and olivine nephelinites erupted around the volcano’s flanks. The nephelinites are extremely low-volume, lowpercentage partial melts of an enriched lithospheric mantle.

Petrology of the magmas

As part of our project, we analyzed rock samples from Capulin, Mud Hill, Baby Capulin, and Sierra Grande for major and trace elements, as well as Sr, Nd and Pb isotopic ratios. The data are shown in Appendix I.

The determination of the magmatic origins of the Capulin basalts is complicated by the fact that the lavas contain abundant xenocrystic (crystals from outside the original magma) sodic plagioclase and quartz grains and xenoliths (foreign fragments) of sandstone, commonly with evidence of melting and mingling with the host basalt. This indicates that the magma has been contaminated by crustal material, quite likely at a high level near the surface. The Dakota sandstone underlies the volcanic rocks throughout the area, and it is the likely source of the quartz and plagioclase grains, which are rounded in shape, more typical of sedimentary rocks than igneous rocks. The contamination changes the chemical composition of the magma, so that it becomes difficult to extrapolate back to the original composition. Even if one picked out the visible xenoliths, there would still be abundant xenocrysts scattered throughout the rock, in addition to the portion that had melted and mixed into the magma. One way to semi-quantitatively assess the effect of the xenocrysts and xenoliths is to compare Capulin and Baby Capulin lava compositions. The Baby Capulin flows, which contain fewer xenoliths and xenocrysts, are 3% lower in SiO_2, richer in iron and magnesium and lower in potassium than those of Capulin are. Similar trends, largely compatible with contamination effects, occur for the trace elements.

The trachybasalts of Capulin and Baby Capulin belong to Stormer's (1972) Capulin basalt series. The data are consistent with magma derivation from an enriched lithospheric mantle source similar to that described by Perry et al. (1987) for the Mount Taylor volcanic field, but with a significant, although undeterminable, amount of crustal contamination.

The basalt of Mud Hill is a transitional basalt, meaning it is on the line between alkaline and sub-alkaline (tholeiitic) basalt. Based on its trace element composition and isotopic ratios, it probably came from relatively shallow melting of enriched mantle lithosphere. Tholeiitic basalts come from higher degrees of melting of mantle than the alkali olivine basalts of the Raton series.

The Sierra Grande andesites are best modeled as the result of mixing of an alkali olivine basalt with a Red Mountain dacite-like magma. Large amounts of basalt ascended under Sierra Grande prior to the construction of the edifice. These basalts formed large volumes of low-K sheet basalts, suggesting a large degree of partial melting of the lithospheric mantle. Heat from these magmas caused partial melting of the lower crust, resulting in the formation of a broadly dacitic magma chamber. As melting in the mantle waned, alkali olivine basalts were generated and ascended to the dacitic magma chambers. These two magmas mixed and differentiated together at the bottom of the crust, and then erupted to form the andesitic lavas of Sierra Grande. As mantle melting lessened, and possibly deepened, the nephelinitic magmas formed and erupted around the flanks of Sierra Grande.

Geochemistry of the magmas

The Capulin basalts are full of Dakota sandstone xenoliths (foreign rock chunks) and xenocrysts (foreign crystals). These are commonly partially resorbed, or melted, and the silica from the quartz grains is clearly a factor in the relatively high amount of silica in the Capulin basalts (50-55% SiO_2), compared with values of 46-50% common in uncontaminated basalts. This contamination means that we cannot filter out one simple process (e.g. crystal fractionation) to get back to the conditions in the mantle where the magma originated. Instead, we must deal with two processes, fractionation and contamination, or unknown individual impacts on the magma. There are no uncontaminated lavas of Capulin age around to use as proxies for a primitive magma. We analyzed a sufficient number of samples from Capulin, Mud Hill, and Baby Capulin to characterize the magma compositions, doing XRF, ICP-MS, and radiogenic isotopic analyses. More analyses would not add to our understanding of the petrologic processes, as they would not take out the geological unknowns.

Our data indicate that the Capulin basalts underwent significant near-surface contamination, incorporating Dakota sandstone and probably underlying sedimentary and crystalline rocks. An ultramafic xenolith found in the Capulin rock collection, thought to be of Capulin origin, is problematic. This is because, if the ascending magma stalled along the way to incorporate significant quantities of country rock, the very dense ultramafic xenolith should have sunk through the magma, and thus not have been erupted. No ultramafic xenoliths were found during our field work, and thus it is at least questionable whether the xenolith came from Capulin, or one of the nearby, uncontaminated volcanic centers.

The significance of Capulin Volcano

Capulin volcano stands out as a unique cinder cone in the lower 48 states and within the National Park Service.

- Capulin's *boca* is uncommon. Most cinder cones erupt lava from their flanks rather than their tops, but the complexity of the way Capulin erupted is most interesting. Its *boca* has many features such as multiple vents, lava lakes and collapsed lava tubes. Luckily, a large part of the *boca* is preserved within the current park boundary. We strongly recommend the creation of a new interpretive trail in the *boca*.

- Capulin's road, for better or for worse, allows even the most casual visitor an excellent vantage point from which to view the geology of the area. The rim trail allows visitors to view Capulin's flows and the major elements of the RCVF.

- The volcano has long been a stop for university geology field trips. It is near major highways, is well preserved, has always been accessible, and now its geology has been studied more carefully.

- The educational potential of the park has always been strong. The opportunity now exists for the park to promote itself even more as a site for geological education and further research.

Recommendations for Future Work

- A good geoengineering survey of the road up the volcano is called for. This might produce suggestions on how to minimize the current high rate of erosion of the cone due to the road's presence.
- Rangers should keep their eyes open for a location where the lava flow was emplaced on top of Dakota sandstone and baked the sandstone to a noticeable red. This would be a potential candidate for thermoluminescence dating.
- Ecological survey to determine what is there, and how best to manage it.

- "Rubber-sheeting" of the aerial photographs to more closely coincide with the digitized data. This would require the addition of ArcView Spatial Analyst and Image Analyst to ArcView GIS 3.1. ArcView could also be upgraded to version 3.2, which came out in August 1999.
- Determine the number of vents in the area.
- Determine more precisely the volumes of the different flow series.

References

Baldridge, W. S., Olsen, K. H., and Callender, J. F., 1984. Rio Grande rift, problems and perspectives, in Baldridge, W. A., Dickerson, P. W., Riecker, R. E., and Zidek, J., eds., Rio Grande rift, northern New Mexico, New Mexico Geological Society Guidebook 35, 1-12.

Baldwin, B., and Muehlberger, W. R., 1959. Geologic studies of Union County, New Mexico, New Mexico Bureau of Mines and Mineral Resources Bulletin 63, 171 pp.

Cerling, T.E., 1990. Dating geomorphologic surfaces using cosmogenic ^{3}He. Quaternary Research, 33, 148-156.

Chapin, C. E., and Kelley, S. A., 1997. The Rocky Mountain erosion surface in the Front Range of Colorado, in, Bolyard, D. W., and Sonnenberg, S. A., eds., Geologic History of the Colorado Front Range, Rocky Mountain Association of Geologists, 101-113.

Dolliver, P. N., 1990. Pre-Coyote Creek landscape and high plains origins, in, Bauer, P. W., Lucas, S. G., Mawer, C. K., and McIntosh, W. C., eds., Tectonic development of the southern Sangre de Cristo Mountains, New Mexico, New Mexico Geological Society 41st Annual Field Conference, 73-75.

Dungan, M. A., Thompson, R. A., and Stormer, J. S., 1989. Rio Grande rift volcanism: Northeastern Jemez zone, New Mexico, in Chapin, C., and Zidek, J., eds., Field excursions to volcanic terranes in the western United States, volume 1: Southern Rocky Mountain region. New Mexico Bureau of Mines and Mineral Resources Memoir 46, 475-483.

Hyndman, D. W.,1985. Petrology of igneous and metamorphic rocks, McGraw-Hill Book Company, 786 pp.

Keller, G. R., Karlstrom, K. E., and Farmer, G. L., 1999. Tectonic evolution in the Rocky Mountain region: 4-D imaging of the continental lithosphere, EOS, Transactions of the American Geophysical Union, 80, 493-498.

Kent, H. C., 1972. Review of Phanerozoic History, in Mallory, W.W., editor, Geologic atlas of the Rocky Mountain region, Rocky Mountain Association of Geologists, 56-59.

Kudo, A. M., 1976. A review of the volcanic history and stratigraphy of northeastern New Mexico, in, New Mexico Geological Society Guidebook 27, 109-111.

Kurz, M.M., 1986. In situ production of terrestrial cosmogenic helium and some applications to geochronology, Geochimica et Cosmochimica Acta, 50, 2855-2862.

Mateer, N. J., 1987. The Dakota Group of northeastern New Mexico and southern Colorado, in, Lucas, S. G., and Hunt, A. P., eds., New Mexico Geological Society Guidebook, 38th Field Conference, Northeastern New Mexico, 223-236.

McGookey, D. P., 1972. Cretaceous system, in, Mallory, W.W., editor, Geologic atlas of the Rocky Mountain region, Rocky Mountain Association of Geologists, 190-228.

Nese, J. M., and Grenci, L. M., 1998. A world of weather: Fundamentals of meteorology, Kendall Hunt Publishing Company, 539 pp.

Perry, F.V., Baldridge, W.S. and DePaolo, D.J., 1987. Role of asthenosphere and lithosphere in the genesis of late Cenozoic basaltic rocks from the Rio Grande rift and adjacent regions of the southwestern United States, Journal of Geophysical Research, 92, 9193-9213.

Sayre, W. O., Ort, M. H., and Graham, D., 1995. Capulin volcano is approximately 59,100 years old, Park Science, 15, 10-11.

Stanley, S. M., 1999. Earth System History, W. H. Freeman and Company, 615 pp.

Steven, T. A., Evanoff, E., and Yuhas, R. H., 1997. Middle and late Cenozoic tectonic and geomorphic development of the Front Range of Colorado, in, Bolyard, D. W., and Sonnenberg, S. A., eds., Geologic History of the Colorado Front Range, Rocky Mountain Association of Geologists, 115-124.

Stormer, J.C., Jr., 1972. Mineralogy and petrology of the Raton-Clayton volcanic field, northeastern New Mexico, Geological Society of America, Bulletin, 83, 3299-3322.

Stroud, J. R., 1997. The geochronology of the Raton-Clayton volcanic field, with implications for volcanic history and landscape evolution, New Mexico Institute of Mining and Technology, M. S. thesis, 170 pp.

Trull, T.W., Brown, E.T., Jean-Baptiste, P., 1995. Direct determination of cosmogenic ^{3}He and ^{10}Be production rates in water, Eos, Transactions, American Geophysical Union, 76, 685.

Woodward, L. A., 1987. Tectonic framework of northeastern New Mexico and adjacent parts of Colorado, Oklahoma and Texas, in Lucas, S. G., and Hunt, A. P., eds., New Mexico Geological Society Guidebook, 38th Field Conference, Northeastern New Mexico, 67-71.

Yokoyama, Y., Reyss, J-L., and Guichard, F., 1977. Production of radionuclides by cosmic rays at mountain altitudes, Earth and Planetary Science Letters, 36, 44-50.

Appendices

I. Geochemical data

Analyses at Washington State University were carried out using the following procedure (Table I-1). Approximately 28 grams (g) of fresh chips of the sample are ground in a swing mill with tungsten carbide surfaces for 2 minutes. 3.5 g of the sample powder was weighed into a plastic mixing jar with 7.0 g of spec pure $Li_2B_4O_7$ and, assisted by an enclosed plastic ball, mixed for ten minutes. The mixed powders are fused in graphite crucibles in a muffle furnace at 1000 ^{o}C. After cooling, each bead is reground and the glass powder then refused in the graphite crucibles for 5 minutes. Following the second fusion, the lower flat surface of the cooled beads was ground on 600 silicon carbide grit, finished briefly on a glass plate (600 grit with alcohol), washed in an ultrasonic cleaner, rinsed in alcohol and wiped dry.

The concentrations of 27 elements in the unknown samples are measured by comparing the X-ray intensity for each element with the intensity for two beads each of nine USGS standard samples (PCC-1, BCR-1, BIR-1, DNC-1, W-2, AGV-1, GSP-1, G-2, and STM-1) and two beads of pure vein quartz used as blanks for all elements except Si. The 20 standard beads are run and used for recalibration approximately once every three weeks or after the analysis of about 300 unknowns. The intensities for all elements are corrected automatically for line interference and absorption effects due to all the other elements using the fundamental parameter method. Two standard beads (BCR-P and GSP-1) are run between every 28 unknown samples and so provide a continuing check on instrumental performance. More information on the XRF procedures is available from the Washington State University Geoanalytical Laboratory world-wide web home page:

(http://www.wsu.edu:8080/~geology/pages/services/geolab.htm).

Analytical procedures for the ICP-MS analyses are distinct because rock and mineral samples must be completely dissolved prior to analysis. Samples are first ground in an iron bowl in a shatterbox swing mill. Two grams of this rock or mineral powder is then mixed with an equal amount of $Li_2B_4O_7$ flux, placed into a carbon crucible and fused in a 1000°C muffle furnace for 30 minutes. The resulting fusion bead is briefly ground again in the shatterbox and 250 milligrams (mg) of this powder is dissolved on a hotplate at 110°C, using 6 milliliters (ml) HF, 2 ml HNO_3, and 2 ml $HClO_4$ in an open teflon vial. The sample is evaporated to dryness, followed by an additional evaporation with 2 ml $HClO_4$ at 165°C to convert insoluble fluorides to soluble perchlorates. 3 ml HNO_3, 8 drops H_2O_2, 5 drops of HF and an internal standard of In, Re, and Ru are added to the sample, which is then diluted up to 60 ml final volume (1:240 final dilution). This combined fusion/dissolution procedure ensures the complete dissolution of zircons and other refractory phases such as garnets, while removing silica and boron as matrix elements by volatilizing them as gaseous fluorides.

The instrumentation consists of a Sciex Elan model 250 ICP-MS equipped with a Babington nebulizer, water cooled spray chamber, and Brooks mass flow controllers. Samples are introduced into the argon plasma at 1.0 ml/min using a peristaltic pump and an automatic sampler. Plasma power is 1500 watts. Under these conditions MO^+/M^+ (the proportion of metal ions forming oxides) is minimized. The instrument is run in "multi-element" mode averaging 10 repeats of 0.5 sec/element for a total integrated count time of 5 sec/element. Most elements have more than one isotope.

For these elements the selection of the isotope for measurement is based on relative abundance and freedom from oxide and isobaric interferences.

Unknown samples are run in sets of 17. One acid blank and two samples each of the 3 in-house rock standards BCR-P, GMP-01, and MON-01 are run with each batch, totaling 24 standard and unknown samples per batch. The three in-house standards have been calibrated against 17 international standards. Intensities for standards and unknowns are downloaded to a personal computer and reduced using a conventional spreadsheet program. Raw intensities are corrected for oxide and isobaric interferences and corrected for drift using the In, Re, and Ru internal standards. Calibration curves for each element are then constructed from the six standard samples and single acid blank by plotting given values against the corrected intensities. Concentrations for the unknown samples are then computed from this curve.

Sr, Nd and Pb isotopic ratios were determined by Dr. Ort at University of California, Santa Barbara on a Finnigan MAT 261 multicollector mass spectrometer in static mode. $^{87}Sr/^{86}Sr$ values were normalized within each run to $^{86}Sr/^{88}Sr=0.1194$, and $^{143}Nd/^{144}Nd$ to $^{146}Nd/^{144}Nd=0.7219$. 0.125%/mass unit Pb fractionation factors were applied to all Pb analyses, using NBS-981 as a standard. NBS-987 and Eimers & Amend (E&A) $SrCO_3$ standards were run on each Sr turret and yield average values of NBS-987=0.710210±0.000018 (N=14) and E&A=0.707981±0.000009 (N=4). Ames Nd standards on each Nd turret yield an average analyzed value of 0.511957±0.000005 (N=10). These ratios are similar to those from other laboratories and no additional correction was made. Corrections for in situ decay of ^{87}Rb to ^{87}Sr ranging from 0.000087 to 0.000677 were made using Rb and Sr concentrations. In situ decay of Sm and U was insignificant in the short time since emplacement, based upon Sm/Nd and U/Pb ratios calculated from INAA data, and no age correction was applied.

Table I-1. Average Analyses and Standard Deviation for XRF standards at WSU

	(a) GSP-1		(b) UMAT-1		
Date	Jan-Aug 1997		Oct 1990		
	Average	StDev	Average	StDev	Range
	N=98		N=10 different beads		
Unnormalized Results (Weight %):					
SiO2	68.45	0.18	53.57	0.10	0.31
Al2O3	15.35	0.11	13.48	0.03	0.12
TiO2	0.667	0.004	2.787	0.007	0.019
FeO	3.86	0.01	12.54	0.10	0.38
MnO	0.038	0.001	0.208	0.001	0.003
CaO	2.02	0.01	6.39	0.02	0.06
MgO	1.10	0.10	2.87	0.02	0.06
K2O	5.56	0.09	2.60	0.01	0.02
Na2O	2.91	0.05	3.25	0.02	0.08
P2O5	0.287	0.003	0.885	0.002	0.008
Total	100.24	0.36	98.58	0.19	0.60
Normalized Results (Weight %):					
SiO2	68.29	0.09	54.35	0.06	0.21
Al2O3	15.31	0.07	13.67	0.04	0.11
TiO2	0.666	0.004	2.827	0.007	0.024
FeO*	3.85	0.01	12.72	0.09	0.31
MnO	0.037	0.001	0.211	0.001	0.004
CaO	2.01	0.01	6.48	0.03	0.09
MgO	1.09	0.10	2.91	0.02	0.06
K2O	5.55	0.07	2.64	0.01	0.03
Na2O	2.90	0.05	3.29	0.02	0.06
P2O5	0.286	0.002	0.897	0.003	0.009
Trace Elements (ppm):					
Ni	16	1	0	0	0
Cr	16	2	1	1	3
Sc	4	2	28	3	11
V	54	5	194	4	13
Ba	1294	9	3081	16	51
Rb	253	1	45	1	2
Sr	233	1	275	1	5
Zr	527	1	424	1	3
Y	30	1	47	1	3
Nb	27.4	0.5	26.2	0.8	2.2
Ga	23	1	21	2	6
Cu	31	2	2	2	8
Zn	103	2	123	2	4
Pb	53	2	10	1	3
La	184	10	35	11	40
Ce	399	10	74	5	17
Th	106	2	6	2	5

Table I-2. Geochemical analyses of samples from Capulin Volcano National Monument

Sample ID		SiO2	Al2O3	TiO2	FeO	MnO	CaO	MgO	K2O	Na2O	P2O5	Total	SiO2 nrm	Al2O3 nrm	TiO2 nrm	FeO* nrm	MnO nrm	CaO nrm	MgO nrm	K2O nrm	Na2O nrm	P2O5 nrm
CAV-02	Capulin	54.81	15.75	1.106	7.54	0.129	7.28	5.67	2.06	3.83	0.412	98.58	55.60	15.98	1.122	7.64	0.131	7.38	5.75	2.09	3.89	0.418
CAV-03	Mud Hill	47.67	15.90	1.474	10.60	0.172	9.61	7.69	1.25	3.53	0.586	98.48	48.40	16.15	1.497	10.76	0.175	9.76	7.81	1.27	3.58	0.595
CAV-09	Mud Hill	48.56	15.95	1.429	10.17	0.170	9.48	7.45	1.29	3.53	0.568	98.59	49.25	16.18	1.449	10.31	0.172	9.62	7.56	1.31	3.58	0.576
CAV-15	Baby Capulin	51.54	16.08	1.367	9.96	0.155	7.82	6.44	1.37	3.87	0.387	98.98	52.07	16.25	1.381	10.06	0.157	7.90	6.51	1.38	3.91	0.391

XRF	Ni	Cr	Sc	V	Ba	Rb	Sr	Zr	Y	Nb	Ga	Cu	Zn	Pb	La	Ce	Th
CAV-02	82	132	15	142	929	30	711	166	19	28.9	18	36	69	7	34	55	8
CAV-03	112	188	31	196	622	16	†813	167	26	27.4	20	61	87	5	33	58	3
CAV-09	102	183	27	194	660	14	†820	168	25	28.8	20	49	89	5	47	64	4
CAV-15	95	153	23	171	618	16	592	153	22	22.0	16	42	87	3	28	49	4

ICP-MS	La	Ce	Pr	Nd	Sm	Eu	Gd	Tb	Dy	Ho	Er	Tm	Yb	Lu	Ba	Th	Nb	Y	Hf	Ta	U	Pb	Rb	Cs	Sr	Sc
CAV-02	37.62	63.91	6.68	25.61	4.98	1.57	4.46	0.68	3.86	0.75	1.94	0.28	1.68	0.27	897	5.73	28.63	20.35	3.60	1.91	2.15	8.43	29.6	0.57	716	20.1
CAV-03	41.07	73.72	8.08	31.87	6.51	2.09	5.88	0.89	5.22	1.03	2.69	0.37	2.19	0.34	601	3.06	26.29	27.23	3.55	1.53	0.89	4.40	19.0	0.23	820	30.0
CAV-09	39.69	70.45	7.71	30.59	6.19	1.99	5.47	0.85	4.99	0.98	2.49	0.36	2.13	0.34	621	3.26	26.30	25.77	3.51	1.54	0.95	4.66	17.1	0.27	790	28.4
CAV-15	29.07	51.57	5.60	22.07	4.86	1.60	4.66	0.73	4.41	0.88	2.32	0.31	1.93	0.31	600	3.33	20.34	23.23	3.39	1.30	1.22	5.39	19.3	0.33	593	23.3

Table I-3. Microprobe analyses of Capulin xenolith. This xenolith is from the Capulin Volcano National Monument collection, reputedly gathered at the monument, but no sampling location is known.

	CPX1	CPX2	OPX1	OPX2	Spinel 1	Spinel 2	Olivine 1	Olivine 2
SiO_2	51.45	51.68	55.19	54.65	0.14	0.14	41.99	41.41
TiO_2	0.44	0.35	0.06	0.12	0.13	0.12	0	0
Al_2O_3	6.72	7.02	5.16	5	54.95	53.97	0.03	0.03
Cr_2O_3	0.98	1.01	0.48	0.44	13.32	13.43	0	0.02
FeO	3.17	3.27	6.17	6.17	11.32	11.4	9.81	9.68
MnO	0.06	0.07	0.11	0.19	0.14	0.06	0.13	0.18
MgO	14.73	15.14	30.55	30.62	20.14	19.86	47.53	47.15
CaO	19.22	19.97	1.01	1.04	0	0.02	0.18	0.13
K_2O	0	0	0	0	0	0	0	0.02
Na_2O	1.36	1.18	0.16	0.13	0	0.05	0.02	0.03
Total	98.13	99.69	98.89	98.36	100.15	99.06	99.69	98.64
Mg/(Mg+Fe)	0.892	0.892	0.898	0.898				
En	48.6	48.3	87.9	87.9				
Wo	45.6	45.8	2.1	2.1				
Fs	5.9	5.9	10	9.9				

Table I-4. Isotope data from Capulin Volcano National Monument

Lab ID	Sample ID	Location	$^{206}/^{204}Pb$(raw)	$^{207}/^{204}Pb$(raw)	$^{208}/^{204}Pb$(raw)	$^{206}/^{204}PB$ (Red.)	$^{207}/^{204}PB$ (Red.)	$^{208}/^{204}PB$ (Red.)	$^{143}Nd/^{144}Nd$	Nd errors	e_{Nd}	$^{87}Sr/^{86}Sr$	Sr errors	$^{87}Sr/^{86}Sr$ normalized to NBS=0.710235	Standard values during runs shown at sample before which it was run.
A-1	SG-14	Sierra Grande	17.557	15.406	37.133	17.601	15.464	37.319	0.512467	0.000007	-3.34	0.704348	0.000012	0.704418	NBS=.710173±26;.710164±10; AMES=.511891±14
A-2	SG-13cc	Sierra Grande	18.039	15.452	37.608	18.084	15.510	37.796	0.512579	0.000008	-1.15	0.704615	0.000017	0.704685	
A-3	SG-14acc	Sierra Grande	18.259	15.466	37.948	18.305	15.524	38.138	0.512707	0.000008	1.35	0.704141	0.000017	0.704211	
A-4	CAV0-10	Capulin	17.563	15.411	37.159	17.607	15.469	37.345	0.512665	0.000009	0.53	0.704016	0.000013	0.704086	AMES=.511897+15
A-5	CAVO-15	Baby Capulin	17.556	15.409	37.131	17.600	15.467	37.317	0.512693	0.000008	1.07	0.703883	0.000010	0.703953	AMES=.511905+6
A-6	CAVO-16	Clayton, E of Cap.	17.984	15.449	37.603	18.029	15.507	37.791	0.512596	0.000012	-0.82	0.704251	0.000016	0.704321	AMES=0.511891±8 for A-5 and B-1

REPORTABLE ERRORS:
Sr=0.000020
Nd=0.000015
8/4Pb=.01-.03
6/4,7/4=.005

II. Age determination data

Table II-1. Cosmogenic ^{3}He Surface Exposure Age of Raton Clayton Olivine

Location	Phase	crushed $^{3}He/^{4}He$ (R/R_A)	[He] (10^{-9} ccSTP/g)	Phase	melted $^{3}He/^{4}He$ (R/R_A)	[He] (10^{-9} ccSTP/g)	$^{3}He_c$ (10^{-12} ccSTP/g)
Lat 36°47'N Long 103°58'W 7350 ft. a.s.l	olivine crystals (772.5 mg)	7.05 ± 0.25	2.45	olivine powder (758.7 mg)	239.9 ± 2.4	3.48	1.13

Notes:

- $^{3}He_C$ = $[^{3}He]_{melt}$ - $[^{3}He]_{initial}$ = $[^{4}He]_{melt}$ $\{(^{3}He/^{4}He)_{melt}$ - $(^{3}He/^{4}He)_{crush}\}$.
- $^{3}He_c$ = $(3.48\times10^{-9})\{(239.9 - 7.05)(1.39\times10^{-6})\}$ = 1.13×10^{-12} ccSTP/g, where 1.39×10^{-6} is the atmospheric ratio.
- The production rate at sea level at this latitude is ~118 atoms/g/y (Trull et al., 1995) (=4.39×10^{-18} ccSTP/g/y).
- The exposure age for this production rate is T = 257,000 years.
- *The Elevation Correction*
  - ◊ $J^{3}{}_{He^*}(z) = J^{3}{}_{He^*}(z=0)\{\exp[-(x-1013)/L]\}$, where x is the atmospheric depth in g/cm^2 (x=1013.25 at sea level), z is elevation above sea level, and L is the attenuation length for cosmic radiation in the atmosphere (L=160 g/cm^2) (Kurz, 1986).
  - ◊ For z=7350 ft. (2240 m), x = 786 g/cm^2, and $J^{3}{}_{He^*}(z)$ = 4.13 $J^{3}{}_{He^*}(z=0)$ @ 488 atoms/g/y.
  - ◊ The elevation-corrected exposure age is 62,300 years. The uncertainty is on the order of 10% (or more), primarily as a result of uncertainty in the production rate.

Table II-2. The elevation correction for cosmogenic ^3He surface exposure age determinations, from Yokoyama et al. (1977).

z (m)	x (g/cm^2)	J/J(z=0)
0	1013	1.000
500	973	1.455
1000	916	2.078
1500	862	2.912
2000	810	4.030
2500	761	5.474
3000	714	7.343
3500	670	9.667
3840	640	11.661
4000	628	12.569
5000	551	20.338
6000	481	31.500
7000	419	46.409
8000	363	65.858

Other Project Materials

Geologic map on Zip disk—accuracy to within plus or minus 10 meters. When viewing aerial photographs and geologic themes together, it is apparent that there is an offset. This is primarily due to the method ArcView uses in geo-referencing aerial photographs. Final map submitted July 1999.

Specimen Lists

Dr. Ort's Specimen list (all samples less than 2 kg)

Sample Number	Description	Location
CAVO-1	sandstone xenolith from Boca	NW.NE.NE 5, T29N, R28E
CAVO-1	squeezeup, northern Boca	SW.NW.SW 33, T30N, R28E
CAVO-3	lower flow at mouth of Mud Hill	SE.NE.NE 33, T30N, R28E
CAVO-4A	spatter agglomerate, Mud Hill	NW.NW.NW 34, T30N, R28E
CAVO-4B	blocky scoria, phreatomagmatic, Mud Hill	NW.NW.NW 34, T30N, R28E
CAVO-5A	spatter east of Mud Hill	SE.NE.SE 28, T30N, R28E
CAVO-5B	Sample with ash in it, east of Mud Hill	SE.NE.SE 28, T30N, R28E
CAVO-7	lava from linear hill east of Mud Hill	SE.SE.SW 27, T30N, R28E
CAVO-8	olivine-pyroxene basalt east of Mud Hill	SW.SW.SE 27, T30N, R28E
CAVO-9	Capulin lava flow just below Mud Hill	NE.NW.SW 27, T30N, R28E
CAVO-10	samples from collapsed lava tube south of Capulin volcano	NE.SE.SE 7, T29N, R28E
CAVO-15	scoria from spatter cone just south of Baby Capulin	SW.NW.NW 26, T30N, R28E
CAVO-16	sample from "spring" hill 2-3 km east of Capulin volcano	NW.NW.NW 2, T29N, R28E
CAPM–1	Paleomagnetism site on Capulin south flow (8 cores)	SE.SW.SE 8, T29N, R28E
CAPM-2	Paleomagnetism site on Capulin west flow (8 cores)	NW.NE.SE 32, T30N, R28E
CAPM-3	Paleomagnetism site on Capulin cone south spatter rim, south side (8 cores)	SE.SW.NW 4, T29N, R28E

Dr. Sayre's specimen list (all are large hand samples)

Sample Number	Description	Location
CAVO 1	Capulin basalt from west side of hill #1, showing shear layering in vesicle size	591,145 E 4,071,136 N

CAVO 2	Fragment of bomb (cooling cracks on surface) with altered sandstone xenolith from north side of hill #1	591,297 E 4,071,232 N
CAVO 3A and B	Two fragments of basalt with altered sandstone xenolith from north side of hill #1	591,297 E 4,071,232 N
CAVO 4A and B	Two fragments of basalt interfingering (less than 2 cm layers) with altered sandstone from north side of hill #1	591,297 E 4,071,232 N

Park Science Article

Capulin Volcano is approximately 59,100 years old, v. 15, no. 2, spring, 1995, p. 10-11.